Computer Simulation of Flow and Heat Transfer During Processing of Polymers, Heavy Corn Syrup and Defatted Soy Flour in Single-Screw Extruders

by

Gagan Ghai

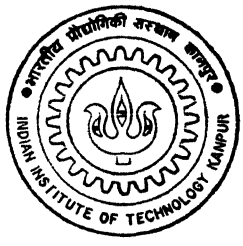

DEPARTMENT OF MECHANICAL ENGINEERING

INDIAN INSTITUTE OF TECHNOLOGY KANPUR

March, 1996

Computer Simulation of Flow and Heat Transfer During Processing of Polymers , Heavy Corn Syrup and Defatted Soy Flour in Single-Screw Extruders

A Thesis Submitted

in Partial Fulfilment of the Requirements

for the Degree of

Master of Technology

by

Gagan Ghai

to the

DEPARTMENT OF MECHANICAL ENGINEERING

INDIAN INSTITUTE OF TECHNOLOGY, KANPUR

March, 1996

CERTIFICATE

It is certified that the work contained in the thesis entitled, "*Computer Simulation of Flow and Heat Transfer During Processing of Polymers , Heavy Corn Syrup and Defatted Soy Flour in Single-Screw Extruders*", by Mr *Gagan Ghai* has been carried out under my supervision and that this work has not been submitted elsewhere for a degree.

P. S. Ghoshdastidar

(Dr. P. S. Ghoshdastidar)
Associate Professor
Department of Mechanical Engineering,
Indian Institute of Technology,
Kanpur.

March,1996

ME- 1996-M-GHA-CEM

Dedicated to

my Parents

the metering section. Comparison of numerical results with available experimental data reveals the reliability of power-law model for higher moisture content dough as compared to lower moisture content or drier doughs.

ACKNOWLEDGMENTS

I express my deep gratitude and indebtedness to Dr. P.S. Ghoshdastidar for his invaluable guidance and suggestions through out this work.

Particular thanks are due to Dr. R.P. Chhabra, Chemical Engineering Dept., IIT Kanpur for sending the book entitled, "Extrusion of Foods", by J.M. Harper from University of New South Wales,Australia and Dr. N.S. Vyas, Mechanical Engineering Dept., IIT Kanpur for sending the M.S. Thesis of D.S.C. Fong from Virginia Polytechnic Institute and State University, Blacksburg, Virginia, U.S.A. without which this thesis could not have been completed.

The financial support of this research, by the Extramural Research Division II of Council of Scientific and Industrial Research, New Delhi, is greatly appreciated.

Finally, I would like to extend my gratitude to my family and my friends for providing suggestions and encouragement at every stage through out the work.

NOMENCLATURE

b	temperature coefficient of viscosity
C_p	specific heat of the fluid at constant pressure
D	barrel inner diameter
G	Griffith number $= \bar{\mu}\ V_{bz}^2/[K_f(T_b - T_i)]$
H	height of the screw channel
H_d	depth (below the screw surface) at which the coordinate system is fixed
K_f	thermal conductivity of the fluid
K_s	thermal conductivity of the screw material
L	axial screw length(metering section)
N	screw speed, r.p.m.
n	power law index
p	pressure
$\bar{p}$	reference pressure $[= \bar{\mu}\ (V_{bz}/\mathrm{H})]$
p_{av}	average pressure in the x-y plane at each z-location
Pe	Peclet number $(= V_{bz}\mathrm{H}/\alpha)$
Q	total volumetric flow rate
q_v	dimensionless volumetric flow rate or throughput parameter $[= \mathrm{Q}/\mathrm{HW}V_{bz}]$
T	temperature
T_i	temperature at the inlet of the heating zone

T_o	reference temperature
u	velocity component in x direction
V_b	tangential velocity of the barrel (= πDN/60)
V_{bx}	component of V_b along x [= $V_b \sin\phi$]
V_{bz}	component of V_b along z [= $V_b \cos\phi$]
v	velocity component in y direction.
W	width of screw channel.
w	velocity component in z direction
x	coordinate axis normal to screw flight.
y	coordinate axis normal to screw root.
z	coordinate axis along the screw channel.

Greek Symbols

α_f	thermal diffusivity of the fluid = [$K_f/\rho C_p$]
β	non-dimensional b [= b(T_b-T_i)]
$\dot{\gamma}$	strain rate [= $\{2(\frac{\partial u}{\partial x})^2 + (\frac{\partial v}{\partial y})^2\} + (\frac{\partial v}{\partial x} + \frac{\partial u}{\partial y})^2 + (\frac{\partial w}{\partial y})^2 + (\frac{\partial w}{\partial x})^2]^{1/2}$
$\dot{\gamma}^*$	dimensionless strain rate [= $\dot{\gamma}H/V_{bz}$]
$\dot{\gamma}_o$	reference strain rate
θ	dimensionless temperature [= (T - T_i)/(T_b - T_i)]
θ_{bulk}	dimensionless local bulk or average fluid temperature [=$(1/q_v) \int_{H_d/H}^{1+H_d/H} w^* \theta_f dy^*$]
μ_o	reference viscosity
$\bar{\mu}$	average viscosity as defined in Eqs. (2.8), (2.10) and (2.12)
μ^*	non-dimensional viscosity = $\mu/\bar{\mu}$
ρ	density of fluid
ϕ	screw helix angle

Subscript

b	barrel
dev	developed
f	fluid
i	inlet
o	reference quantity
ref	reference quantity
s	screw

Superscript

*	dimensionless quantity

Contents

List of Tables

List of Figures

Chapter 1

INTRODUCTION

1.1 Introduction

The process of extrusion consists of converting a suitable raw material into a product of specific cross-section by forcing the material through an orifice or die under controlled conditions. Screw extrusion, one such process, is used in many industries such as those related to plastics, polymers, pharmaceuticals and food products. In order that this conception has practical value, some requirements must be satisfied both as regards the equipment and the raw material. The equipment must be capable of providing suitable pressure, continuously and uniformly, on the material so that it attains required properties. Thus it is necessary to understand the underlying mechanism and determine heat transfer rates, residence time distribution and the thermal and fluid flow fields etc. within the extruder.

The screw extrusion machine (Fig. 1.1) consists of a screw of special form rotating in a closely fitted heated barrel or cylinder in which feed port is placed radially or tangentially at one end and an orifice or die axially at the other. It usually has three different geometric sections: a feed section with relatively deep channel depth or flights with greater than normal pitch, a tapered compression or

transition section - where temperature and pressure are raised, and a relatively shallow metering section of constant depth - where temperature and pressure increases further and high pressure enhances mixing.

1.2 Fundamental Differences between Polymer and Food Processing

Although there are quite a few similarities between food and polymer extrusion, there are some points in which they distinctly differ. They are as follows:

1. A polymer (or a thermoplastic) can be melted and then on solidification the original material can be restored Thus the process is reversible. On the other hand, there are irreversible cooking reactions in the food processing.

2. The cooking of food inside an extruder is a complicated process. Both chemical and physical changes may occur at the same time under the influence of moist heat, pressure and shear. Two most important reactions in food extrusion are protein denaturation and starch gelatinisation.

3. The dough viscosity greatly increases as the reaction proceeds. In contrast, the apparent viscosity of thermoplastic will usually decrease as the temperature increases.

Remsen and Clark (1978) found that for a 25% soy flour suspension, the apparent viscosity did decrease initially upon heating until around 160°F(71.11°C) and then the viscosity started to increase because of denaturation reaction (here the starch gelatinisation reaction is unimportant) demonstrating the cooking phenomenon. Thus, during cooking the dough will first encounter "melting" with a decrease in viscosity until a critical temperature is reached at certain point down the channel

when its apparent viscosity will show a rise. In short, the viscosity of a food system is not only a function of shear rate and temperature, but also depends on the composition and the time-temperature history of the process.

Thus it is in the terms "melting" and "cooking" that the analogy between a food and plasticating extruder stops.

1.3 Literature Review

Although extrusion as a manufacturing process for structural material can be considered to have originated at the end of 19th century, it is only within the last 50 years or so its full potential has begun to be realised. First reported industrial machine for extrusion of lead pipe was constructed by John Bramah in 1795. From then until the invention of specially designed thermoplastic extruder in 1953 by Paul Troester in Germany, the process has been used extensively for gutta percha, rubber, cellulose nitrate and casein (Fisher, 1954). Early progress was mainly based on 'cut and try' basis and the fundamental process was not fully understood.

In recent years experimental and numerical studies have been done to understand the transport phenomena in the extrusion process, resulting in much scientific knowledge, primarily for single screw extruders. The first theoretical research on plasticating extruder was done by Rowell and Finlayson (1922). Most of the initial research (Tadmor and Gogos, 1979, Fenner, 1979, Tadmor and Klien, 1970)was preliminary in nature and relates to the extrusion of polymers. Griffith (1962) solved for fully developed flow of an incompressible power-law fluid in a screw extruder. The velocity and temperature are essentially the same as those in channel of infinite width and length. The effects of curvature and leakage across the flights were also ignored. Marshall et al. (1965) and Palit(1974) reported detailed experimental results obtained from extruders processing materials such as LDPE,

polypropylene, polyvinylchloride, which showed screw surface temperatures rising rapidly along the feed and compression section to steady values slightly higher than the barrel temperature along most of the metering section. Zamodits and Pearson (1969) obtained numerical solutions for a fully developed 2-D non-Newtonian flow of polymer melts in infinitely wide rectangular screw channels, taking into account the effect of transverse flow and superimposed steady temperature profile. Bigg and Middleman (1974) and Lidor and Tadmor (1976) have performed theoretical analysis to determine the residence time distribution function and strain distribution in screw extruders Tadmor and Gogos (1979) and Fenner (1979) have solved the flow of a polymer in the feed, compression and metering section of an extruder. Fenner (1977) also solved the case of temperature profile developing along the length of screw channel. Agur and Vlachopolous (1982) have studied the flow of polymeric materials, which included a model for the flow of solids in hopper, a model for solid conveying zone and a model for melt conveying zone. Mokhtarin and Erwin (1982) developed a mathematical model for mixing in a single screw extruder. Lawal and Kalyon (1993) included wall slip in numerical calculation. Gupta et al. (1992) have developed a 3-D finite element model for incompressible flow of non-Newtonian fluids which can be applied to simulation under isothermal condition. Karwe and Jaluria (1990) have numerically analyzed by finite difference techniques the flow of polymeric material in metering section of single screw extruder. Sastrohartono et al. (1995) developed a numerical model of 3-D transport associated with plastic extrusion in a single screw extruder using finite element scheme and compared the numerical results satisfactorily with experiments done by them. As predicted by Das and Ghoshdastidar (1994a,b) the results of Sastrohartono et al. (1995) clearly indicate the inadequacies of 2-D modelling.

The quasi 3-D steady state model developed by Das and Ghoshdastidar (1994b) considers cross thermal convection, i.e. convections normal to screw flights and

screw roots, and coupled heat transfer in the melt and the screw. The model is for the metering section. The flow is assumed to be hydrodynamically developed but thermally undeveloped.

In food extrusion rheology, the key issue is obtaining the useful data. As pointed out by Schwartzberg (1979), the essential difficulty in measuring dough rheology is that rheological properties are affected by kinetic phenomenon, such as cross linking and protein breakdown. One possible solution, as suggested by Hohner (1978) is to use multiple dies on an extruder. In this case material with identical histories would be subjected to various shear stresses and corresponding shear rates could be measured. however its use has not yet been reported. Chen et al.(1978), Fong (1978) and Crevone and Harper (1978) obtained flow curves under various temperature and flow rate conditions. From flow curves, rheological properties are inferred. Harper, Rhodes and Wanninger (1971) suggested a logarithmic mixing role form to account for changes in apparent viscosity with changes in moisture and the Arrhenius equation form to correlate with changes in temperature. This model did not take into account changes in apparent viscosity due to cooking of the food. To model time temperature effects on the apparent viscosity of soy protein doughs, Remsen and Clark (1978) applied the work of Roller (1979). This model appeared useful for initial stages of denaturation only. Morgan et al. (1980) have developed a model which describes the effects of temperature-time history, temperature, shear rate, and moisture content on the apparent viscosity of defatted soy flour dough. To evaluate this model, temperature as a function of time is required. No single model exists describing apparent viscosity as a function of composition, variability of ingredients, time, temperature and other extrusion parameters. The power-law model has been used to describe the isothermal flow through the metering section by Harmann and Harper (1974) and Tsao et al. (1978), and for cooking extrusion by Fricke et al. (1977) Once a simple model that describes the important changes

in viscosity that occur with time during cooking of food dough exists, it will be theoretically possible to simulate the entire cooking extrusion process leading to an increased understanding of the principal variables and their influence on extrusion rate, energy input and finished product characteristics (Harper, 1978).

1.4 Objectives of the Present Study

The objectives of present study are two-fold.

First Part

1. To extend the quasi 3-D model of Das and Ghoshdastidar (1994b) to non-power law polymer like Viscasil and compare the numerical results with the experimental results of Sastrohartono et al. (1995). It may be noted that Das and Ghoshdastidar (1994b) did not experimentally validate their numerical model However recently, Das and Ghoshdastidar (1996) successfully validated their results for power-law fluids such as LDPE with the experimental work of Pahl(1974).

2. To extend the quasi 3-D model of Das and Ghoshdastidar (1994b) to a Newtonian fluid (which is also a food) such as heavy corn syrup for which the viscosity model is available in Sastrohartono et al. (1995) and then compare the results for the same screw configuration and input data (dimensional) with LDPE.

Second Part

This part contains the food extrusion modelling. For this, cooking of defatted soy flour dough has been modelled. In the absence of a suitable simple model of viscosity for defatted soy flour dough as discussed in art. 1.3, it is assumed that through out the cooking process the soy flour dough acts like a polymer following power-law

viscosity model. Thus the quasi 3-D model of Das and Ghoshdastidar (1994b) can be used. The input data for 25%, 28% and 33% moisture content defatted soy flour dough have been taken from Fong (1978) to see how good or how bad is the melting approximation through out the cooking process. While the earlier researchers used simple models assuming isothermal flow of power-law food, the present study uses a rigorous quasi 3-D model describing non-isothermal flow of food following power-law viscosity model. The model also takes into account screw conduction

It may be noted that mass transfer is not occurring during extrusion of the soy flour dough This is because of the fact that the discharge pressure in food extruders typically varies between 30 to 60 atm. At these elevated pressures, boiling or flashing of moisture does not occur within the confines of the barrel because the pressure exceeds the vapour pressure of water at the extrusion temperate. Once the food emerges from the die, the pressure is released causing the product to expand with the extensive flashing of moisture. The loss of moisture from the product results in adiabatic cooling of the food materials with the product reaching a temperature of approximately 80°C in a matter of seconds, where it solidifies and sets often retaining its expanded shape (Harper, 1978).

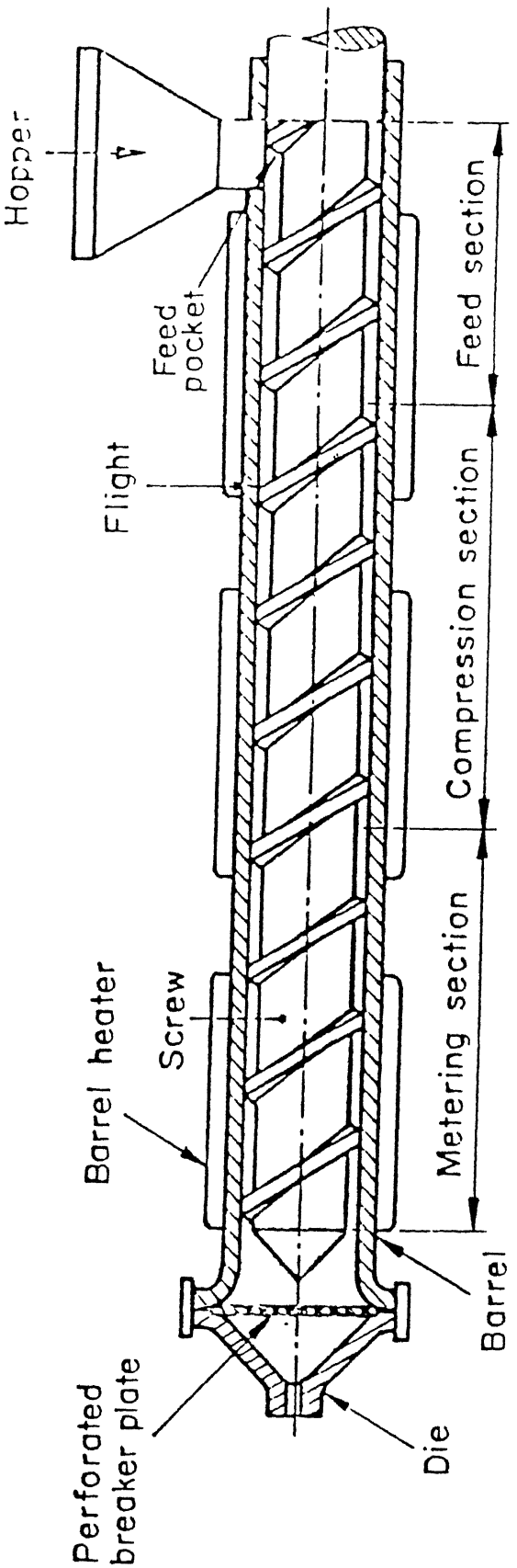

Figure 1 1: A typical single-screw extruder

Chapter 2

THEORY AND BACKGROUND

2.1 Screw Extrusion

In order to predict the flow rates, power consumption, pressure drop, and temperature distribution inside a food extruder, the flow pattern or the velocity profile must be determined.

In a screw extruder materials are constantly being conveyed forward through the rotation of a close fitting screw inside a barrel. It is the drag of the barrel wall on the fluid that will advance the material down the channel in a direction opposite to the rotation. This can be visualised by unwinding the screw channel as shown in Fig.2.1 so that it becomes a straight channel with barrel surface as infinite plane. For ease of analysis the coordinate is fixed to the screw and thus barrel moves in a direction opposite to the screw rotation and its speed V_b is resolved into two components V_{bx} and V_{bz}, the former along the direction normal to the screw flights and the latter along the length of the channel.

The flow pattern inside the channel is composed mainly of four types of flow. The drag flow, is created by the velocity V_{bz} along the helix. It is this component which largely drives the fluid forward. The velocity component V_{bx} creates the transverse

flow. It contributes nothing to the pumping rate but will affect the flow pattern and is responsible for useful mixing. The die or restriction set up at the exit port of the extruder will create the third kind of flow, which sometimes is called back flow or pressure flow. For a very small die opening this flow can be in the reverse direction and might improve mixing in the system. The last type of flow is the leakage flow, which is flow of fluid over the clearance between flights and barrel surface. This flow is generally neglected.

Since our main objective is to predict the pressure and temperature rise which occurs primarily in the metering zone of the screw which is also responsible for high mixing because of its small depth, in this work the flow and heat transfer in the metering section have been analysed in detail. However, a complete model of an extruder must include compression as well as feed section.

2.2 Problem Formulation

2.2.1 Physical Description of the Model

The primary difference between a quasi 2-D model and quasi 3-D model is the inclusion in the latter of the cross-convection terms i.e., thermal convections normal to the screw flights and the base of the screw channel. Similar to the quasi 2-D analysis, the flow is assumed to be hydrodynamically developed but thermally undeveloped. Both the x-boundaries are assumed to be insulated considering that a negligible amount of heat is conducted between the melt and the uncooled screw (Fenner, 1977). Also, 2-D conduction is assumed to be present in the x-y plane of the screw body with both boundaries in the x-direction acting as insulated considering that the screw body is sufficiently thick in that direction. The conjugate heat transfer at the melt-screw interface is modelled by assuming the screw body behaving like one in which small heat conduction is present in a very thin layer below the

screw surface while the rest of the screw remains adiabatic. This assumption is realistic taking into account similar experimental observations by Martin (1970).

2.2.2 Major Assumptions

1. For simplifying the analysis, the coordinate system is fixed to the screw and thus the barrel moves in a direction opposite to the screw rotation.

2. The curvature effects have been neglected as the screw diameter is large as compared to the channel height and therefore the screw is treated as unwound (Fig.2.1).

3. The fluid is considered to be incompressible and flow and heat transfer steady and quasi 3-D.

4. Good thermal contact between melt and metal surface exists.

5 All fluid properties except viscosity are constant.

6. As the screw channel is shallow and long (i.e. small H/W ratio) and also convective effects are small in comparison to viscous effects, creeping flow approximations are made for the conservation of momentum (Schlichting, 1979).

7. The leakage across the screw flights has been neglected.

2.2.3 Governing Equations And Boundary Conditions

Using the above assumptions the governing equations in the non-dimensional form in terms of the dimensionless variables (listed in the Nomenclature) are given below. The length dimensions have been normalised by dividing them by H, velocities by V_{bz} and pressure by $\bar{p}$.

Melt

Continuity:

$$\frac{\partial u^*}{\partial x^*} + \frac{\partial v^*}{\partial y^*} = 0 \tag{2.1}$$

X-momentum:

$$\frac{\partial p^*}{\partial x^*} = 2\frac{\partial}{\partial x^*}(\mu^* \frac{\partial u^*}{\partial x^*}) + \frac{\partial}{\partial y^*}[\mu^*(\frac{\partial u^*}{\partial y^*} + \frac{\partial v^*}{\partial x^*})] \tag{2.2}$$

Y-momentum:

$$\frac{\partial p^*}{\partial y^*} = 2\frac{\partial}{\partial y^*}(\mu^* \frac{\partial v^*}{\partial y^*}) + \frac{\partial}{\partial x^*}[\mu^*(\frac{\partial u^*}{\partial y^*} + \frac{\partial v^*}{\partial x^*})] \tag{2.3}$$

Z-Momentum

$$\frac{\partial p^*_{av}}{\partial z^*} = \frac{\partial}{\partial x^*}(\mu^* \frac{\partial w^*}{\partial z^*}) + \frac{\partial}{\partial y^*}(\mu^* \frac{\partial w^*}{\partial y^*}) \tag{2.4}$$

Energy:

$$Pe(u^* \frac{\partial \theta_f}{\partial x^*} + v^* \frac{\partial \theta_f}{\partial y^*} + w^* \frac{\partial \theta_f}{\partial z^*}) = \frac{\partial^2 \theta_f}{\partial x^{*2}} + \frac{\partial^2 \theta_f}{\partial y^{*2}} + G\mu^* \dot{\gamma}^{*2} \tag{2.5}$$

Screw

Energy:

$$\frac{\partial^2 \theta_s}{\partial x^{*2}} + \frac{\partial^2 \theta_s}{\partial y^{*2}} = 0 \tag{2.6}$$

The viscosity models used in the present study are given in Eq. (2.7), Eq. (2.8) and Eq. (2.9).

The flow in the screw channel is solved in terms of the cross-channel and down-channel flows. The cross-channel flow is defined by u and v velocity components in the x-y plane and while down-channel flow is defined by w velocity component in the z-direction. The cross- and down-channel flow are coupled through μ^* present in Eq. (2.1)-(2.4) for a non-Newtonian case. Here μ^* is a function of local shear rate $\dot{\gamma}^*$, which is invariant of the rate of deformation tensor. In the present case μ^* is:

$\mu^* = \mu/\bar{\mu}$

where μ and $\bar{\mu}$ in the power law model case are of the form:

$$\mu = \mu_o[\frac{\dot{\gamma}}{\dot{\gamma}_o}]^{n-1} exp[-b(T - T_o)] \tag{2.7}$$

$$\bar{\mu} = \mu_o[\frac{V_{bz}}{H\dot{\gamma}_o}]^{n-1} exp[-b(T_i - T_o)] \tag{2.8}$$

in the case of Viscasil are :

$$\mu = \frac{Aexp(\frac{B}{T})}{1 + C[Aexp(\frac{B}{T})\dot{\gamma}]^{1-n}} \tag{2.9}$$

$$\bar{\mu} = \frac{Aexp(\frac{B}{T_i})}{1 + C[Aexp(\frac{B}{T_i})\frac{V_{bz}}{H}]^{1-n}} \tag{2.10}$$

and in the case of Corn syrup :

$$\mu = \mu_o exp[-b(T - T_o)] \tag{2.11}$$

$$\bar{\mu} = \mu_o exp[-b(T_i - T_o)] \tag{2.12}$$

More details of these viscosity models are given in chapters 3 and 4.

The boundary conditions are also obtained in the non-dimensional form as:

at $z^* = 0$,

$$u^* = u^*_{dev}, v^* = v^*_{dev}, w^* = w^*_{dev}, \theta_f = \theta_s = 0 \tag{2.13}$$

For $z^* > 0$

at $y^* = 0$,

$$\frac{\partial \theta_s}{\partial y^*} = 0 \tag{2.14}$$

at the interface, i.e.

at $y^* = \frac{H_d}{H}$

$$u^* = 0, v^* = 0, w^* = 0 \tag{2.15}$$

$$\theta_f = \theta_s, \frac{\partial \theta_f}{\partial y^*} = \frac{K_s}{K_f}\frac{\partial \theta_s}{\partial y^*} \tag{2.16}$$

at the barrel surface, i.e.

at $y^* = 1 + \frac{H_d}{H}$

$$u^* = \frac{V_{bx}}{V_{bz}}, v^* = 0, w^* = 1, \theta_f = 1 \tag{2.17}$$

at $x^* = 0$ and $x^* = \frac{W}{H}$

$$u^* = 0, v^* = 0, w^* = 0, \tag{2.18}$$

$$\frac{\partial \theta_f}{\partial x^*} = \frac{\partial \theta_s}{\partial x^*} = 0 \tag{2.19}$$

The constraint on the flow in the dimensionless form is,

$$\int_0^{W/H} \int_{H_d/H}^{1+H_d/H} w^* dx^* dy^* = \frac{Q}{HWV_{bz}} = q_v \tag{2.20}$$

Here the parameter q_v represents the dimensionless volumetric flow rate also called the throughput emerging from the extruder. These boundary conditions in the dimensional form are shown as in Fig.2.2.

Thus for a given extruder, the parameters that govern the solution are: Pe,G,n,q_v the dimensionless viscosity parameter, β [= b($T_i - T_o$)] and K_s/K_f. Furthermore the pressure P^*_{av} in Eq. (2.4) is a form of space-averaged pressure over x-y plane at any z location.

2.2.4 Method of Solution

A finite volume solution methodology has been adopted. The overall method of solution of the flow field and temperature has been developed following the procedures of Patankar and Spalding (1972), Raithby and Schneider (1979) and Vandoormal and Raithby (1984). A fully implicit scheme is used to march in z^* direction.

2.2.5 Handling of Melt-Screw interface

A discretized energy equation is obtained at the melt-screw interface satisfying the energy equation of the melt and screw (Eq. (2.5) and Eq. (2.6) respectively) and compatibility conditions (Eq. 2.16) following the method of Carnahan et al. (1969). The details can be found in Das (1993).

2.2.6 Overall Solution Algorithm

The overall solution algorithm is shown by a flow chart given in Fig.2.3. The computer program is capable of also predicting correctly the back flow

situations due to smaller die openings (low q_v cases) that frequently arise in case of processing of food doughs.

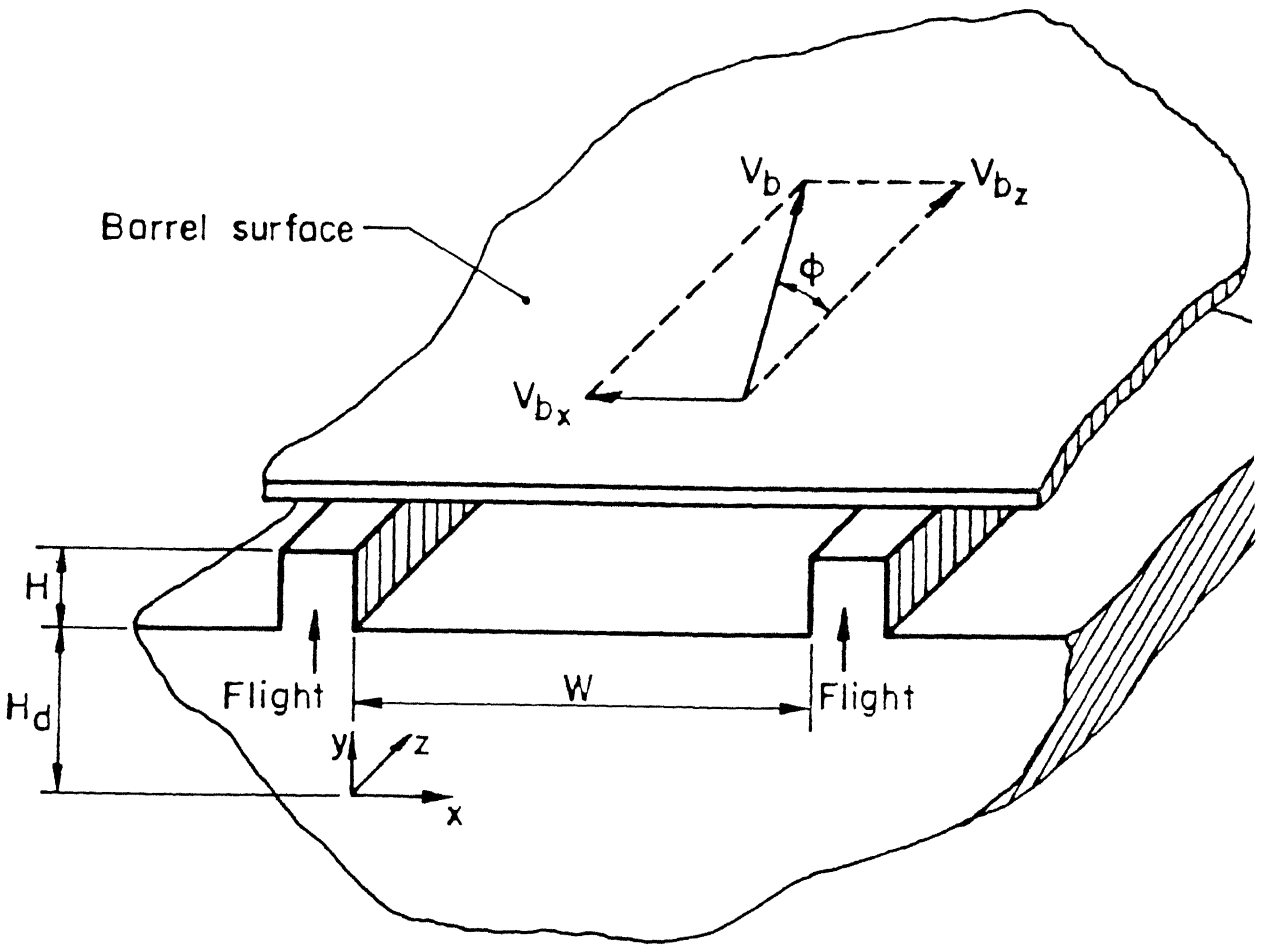

Figure 2 1 Geometry of unwound screw channel

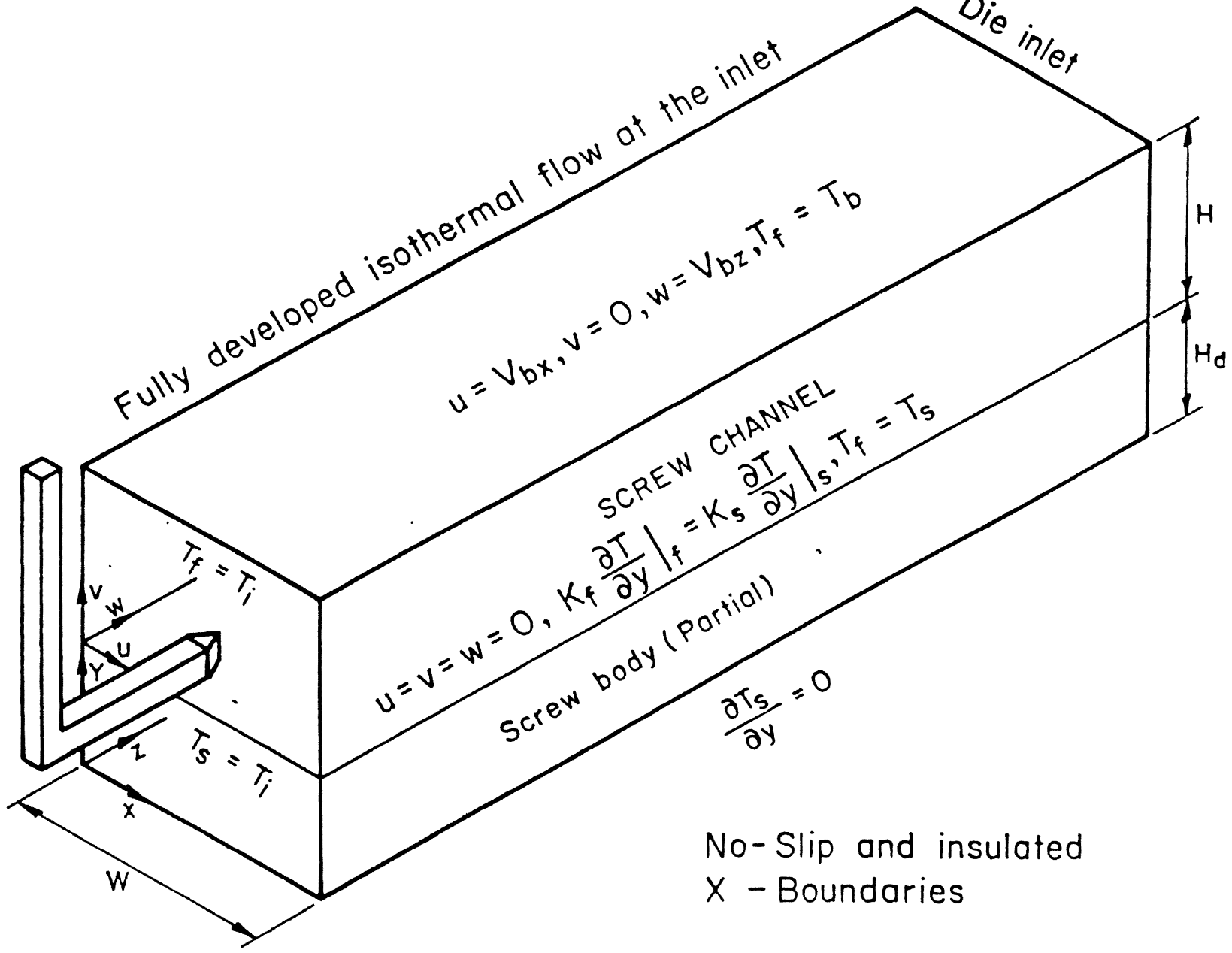
Fully developed isothermal flow at the inlet
Die inlet
$u = V_{bx}, v = 0, w = V_{bz}, T_f = T_b$
SCREW CHANNEL
$u = v = w = 0,\ K_f \frac{\partial T}{\partial y}\Big|_f = K_s \frac{\partial T}{\partial y}\Big|_s, T_f = T_s$
Screw body (Partial)
$\frac{\partial T_s}{\partial y} = 0$
$T_f = T_i$
$T_s = T_i$
H
H_d
W
x
y
z
u
v
w
No-Slip and insulated
X – Boundaries

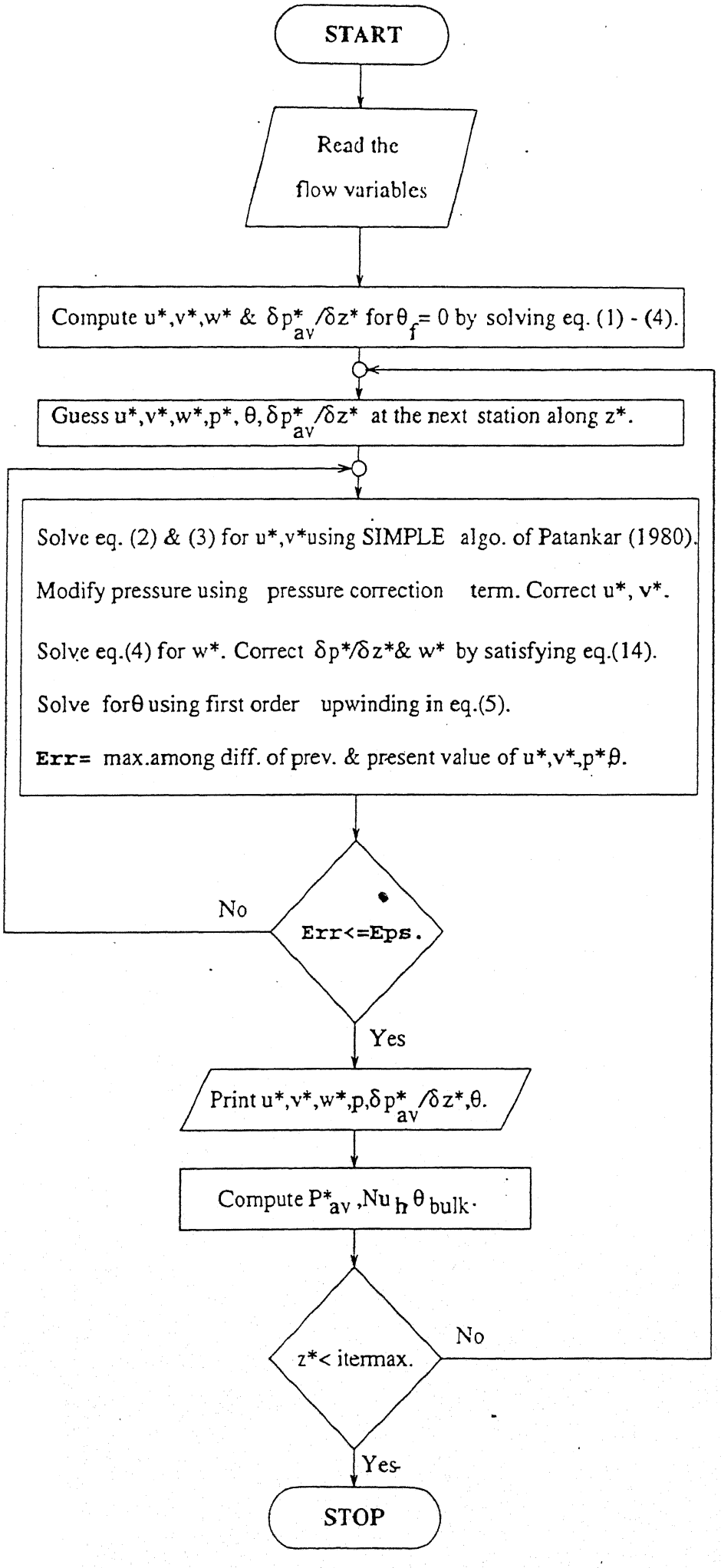

Figure-2.3: Flow chart for the solution algorithm.

Chapter 3

VALIDATION OF THE NUMERICAL RESULTS WITH EXPERIMENTAL RESULTS OF SASTROHARTONO et al. (1995) FOR VISCASIL

3.1 The Viscosity Model

In this chapter, the results based on the quasi 3-D model of Das and Ghosh-dastidar (1994b) are presented for the fluid Viscasil. Like LDPE , Viscasil is also a non-Newtonian fluid. The viscosity model given in Eq.(3.1) for Viscasil 300-M is taken from Sastrohartono et al. (1995). It is a non power-law model.

$$\mu = \frac{Aexp(\frac{B}{T})}{1 + C[Aexp(\frac{B}{T})\dot{\gamma}]^{1-n}} \tag{3.1}$$

where μ is the viscosity in poise, T is the temperature in K, and $\dot{\gamma}$ is the shear rate in s^{-1}. The values of constants for the present case are:

$A = 0.7249023$ poise.

$B = 2560.804$ K.

$C = 7.42082$ x 10^{-5} $(Nm^{-2})^{n-1}$

power law index $n = 0.2671$

Eq.(3.1) is valid over the range of temperatures and shear rates considered here.

3.2 Screw Configuration and Input Data

The Screw Configuration and input data used in present calculation is given in Table 3.1 and the involved dimensionless parameters are given in Table 3.2.

3.3 Results and Discussion

The flow and temperature field over the cross-section at any down-channel position can be studied. Fig.3.1 and Fig. 3.2 show respectively the development of melt temperature θ_f and velocity w^* in z direction along the down channel direction for three z^* locations. It is important to note that θ and w^* are the integrated average quantities over x^*. Due to the heat input at the barrel and the viscous heat dissipation the fluid temperature rises along the channel. This results in decrease in the local viscosity and hence the velocity

Table 3 1. Screw configuration and input data

Screw Diameter, D	30.85 mm.
Pitch	28.0 mm.
Helix angle, ϕ	16.1888°
Maximum channel depth, H	4.7 mm.
Maximum channel width, W	11.52 mm.
Screw tip width	1.924 mm.
Clearance between screw tip and barrel	0.075 mm.
Length of metering section, L	120 mm.
Density, ρ	979 Kg m^{-3}
Thermal Conductivity fluid, K_f	0.155758 $Wm^{-1}K^{-1}$.
Thermal Conductivity screw, K_s (for steel)	45 $Wm^{-1}K^{-1}$.
Specific Heat, C_p	1507.16 $JKg^{-1}K^{-1}$.
Barrel temperature T_b	80^0 C
Screw speed N	60 RPM
Inlet temperature for the metering section T_i	53.8^0 C
Normalized flow rate q_v	0.32

Table 3 2· Dimensionless quantities involved

Peclet number, Pe	4144.176
Griffith number, G	0.012

field changes, since q_v or throughput is maintained constant in the extruder for steady state condition.

The velocity vector plots in Fig 3.3 show a strong recirculating flow across the screw channel which together with down channel velocity results in a spiral motion of the material along the channel. As the material flows the temperature rises due to viscous dissipation and heat input from the barrel. The screw surface temperature and pressure vs. channel length are plotted in Fig. 3.4(a) and Fig. 3.4(b) respectively. It is seen that as expected both continuously increase along the screw channel.

3.4 Experimental Validation for Various Cases

The Experimental results presented here were obtained by Sastrohartono et al. (1995) using a single-screw extruder with a self wiping screw profile. It is to be noted that the screw configuration is same as in Table 3.1.

In the first case barrel temperature $T_b = 25.0°C$, inlet temperature $T_i = 18.9°C$, normalized flow rate $q_v = 0.34$ and screw rotation speed N = 10 rpm.(See Table 3.3). The outlet temperature is the bulk temperature at the exit.

In the second case comparison was done with barrel temperature $T_b = 80°C$ (Table 3.4). The results shown in Table 3.3 and Table 3.4 indicate clearly that the quasi 3-D model is highly reliable.

Table 3 3 Comparison between computed model and experimental results for Viscasil, N = 10 rpm, $T_b = 25\ 0°C$, $T_i = 18\ 9°C$

Test	Outlet Pressure [bars]	Outlet Temperature [°C]
Experimental Results	4.750	24.20
Computed Results	4.854	25.25

Table 3 4 Single-screw extruder characteristic experimental and computed results T_b = 80°C, T_i = 53 8°C; Viscasil-300M

Mass flow Rate [Kgh^{-1}]	Screw speed [rpm]	Outlet Pressure (Experimental) [x $10^5 Nm^{-2}$]	Outlet Pressure (Computed) [x $10^5 Nm^{-2}$]
1.0	10	8.60	8.94
3.6	36	14.31	14.62
6.0	60	18.74	18.96
9.0	90	22.44	22.59

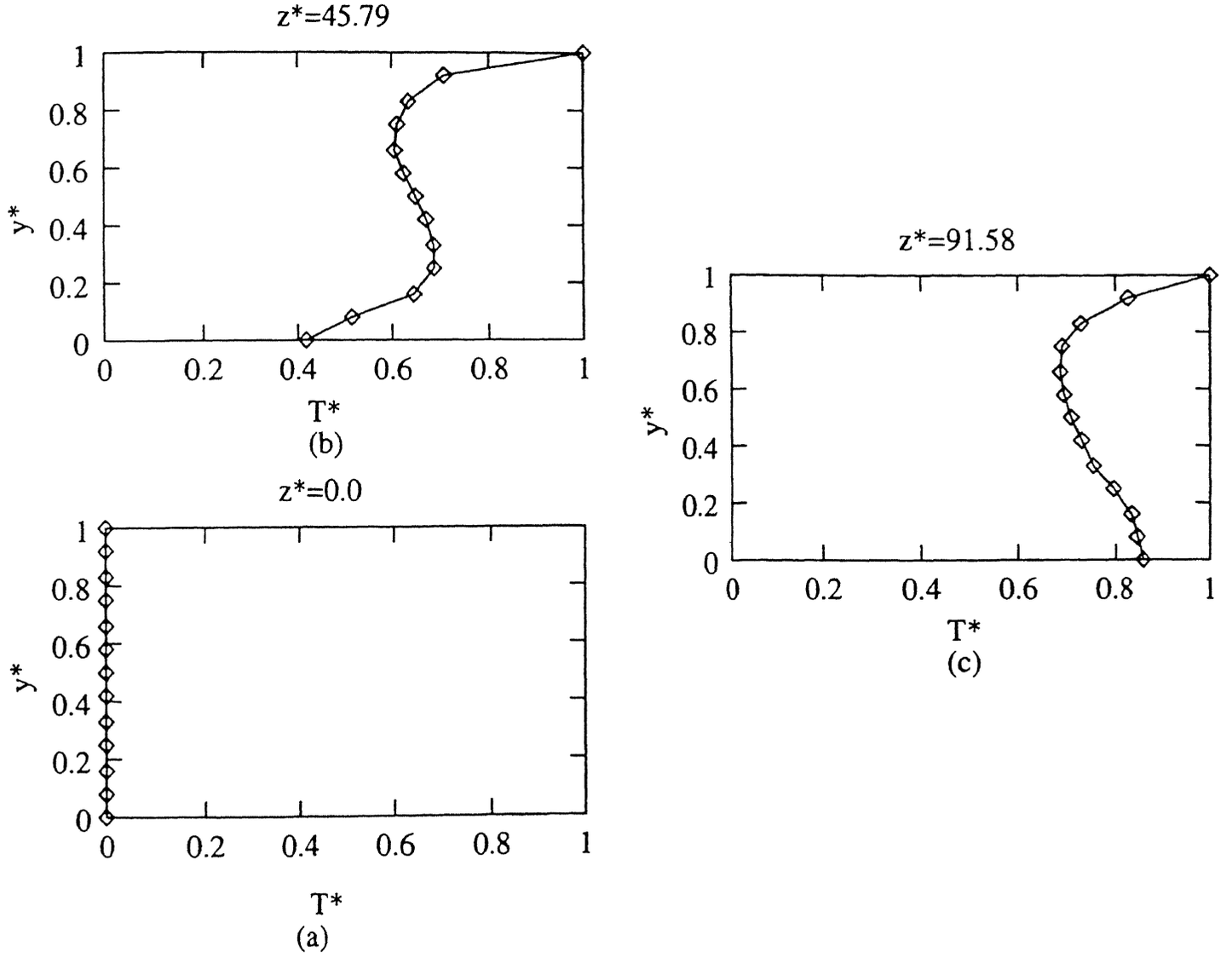

Figure 3.1 Temperature profiles along the screw channel of a single-screw extruder Fluid Viscasil, T_b = 80°C, T_i = 53.8°C, q_v = 0.32, N = 60rpm

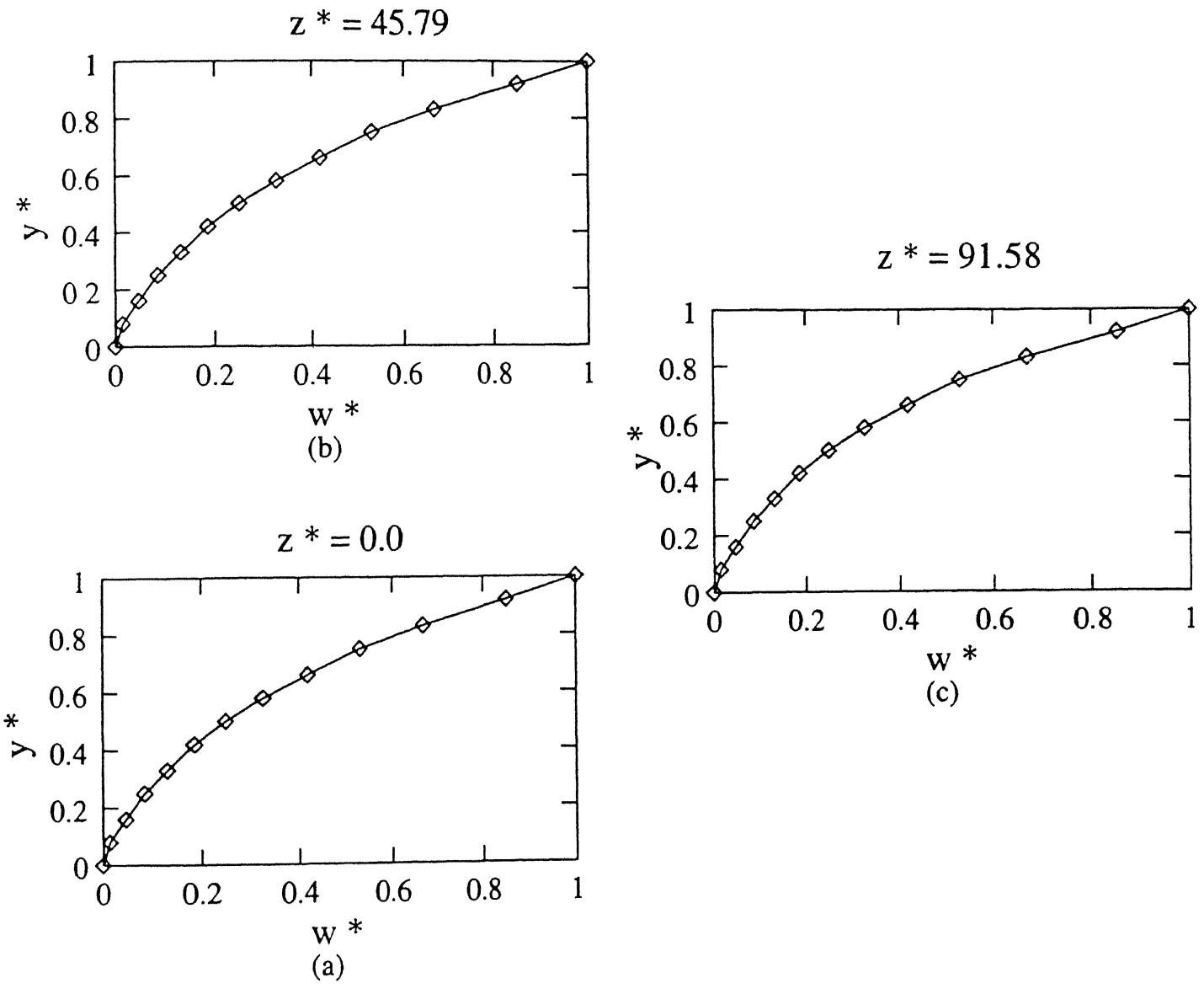

Figure 3 2 w^* profiles along the screw channel of a single-screw extruder Fluid Viscasil, T_b = 80°C, T_i = 53 8°C, q_v = 0 32, N = 60rpm

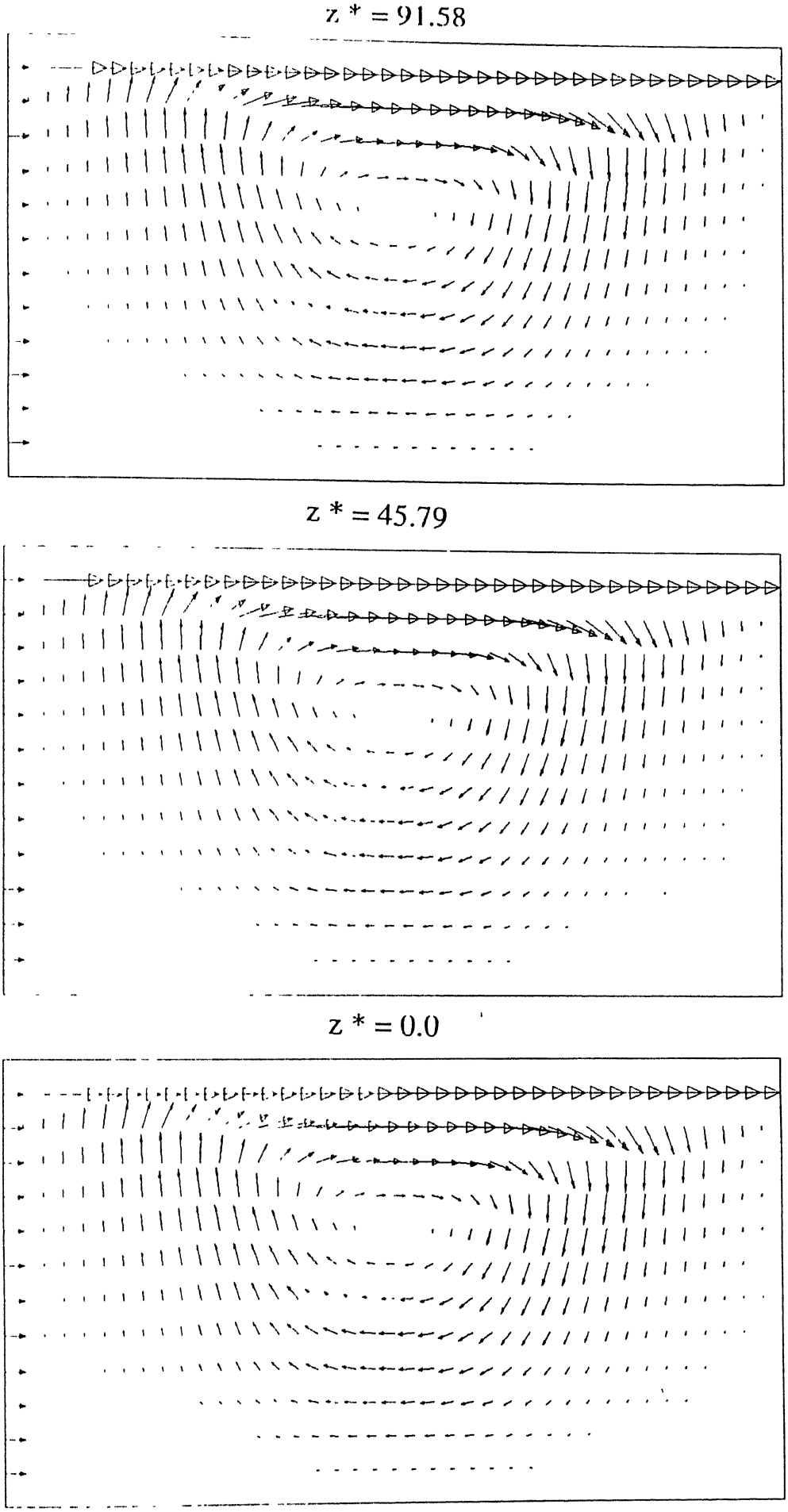

Figure 3 3. Velocity vector plot in cross sectional plane at 3 downstream location for quasi 3-D model

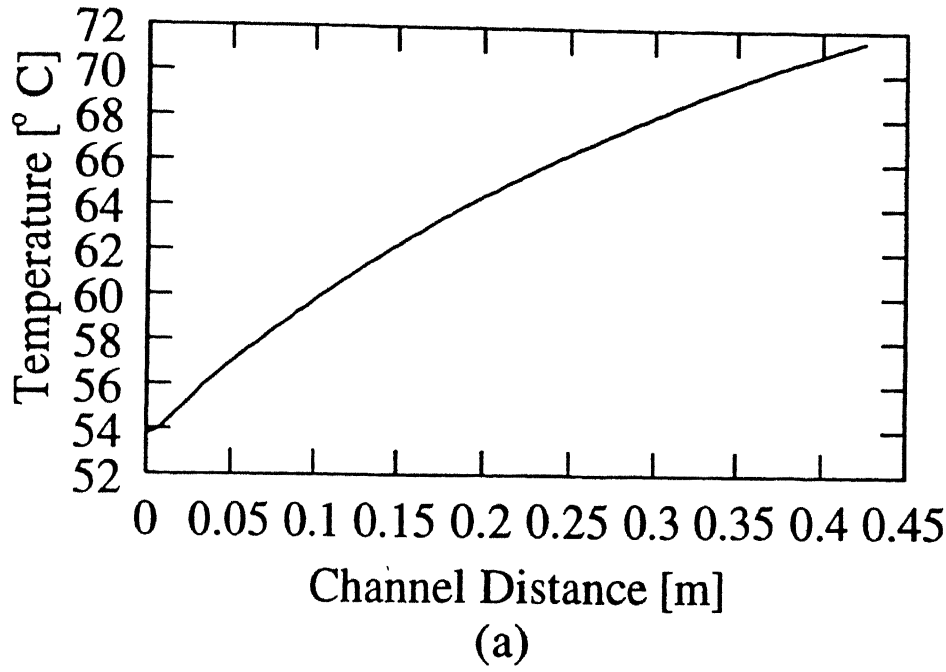

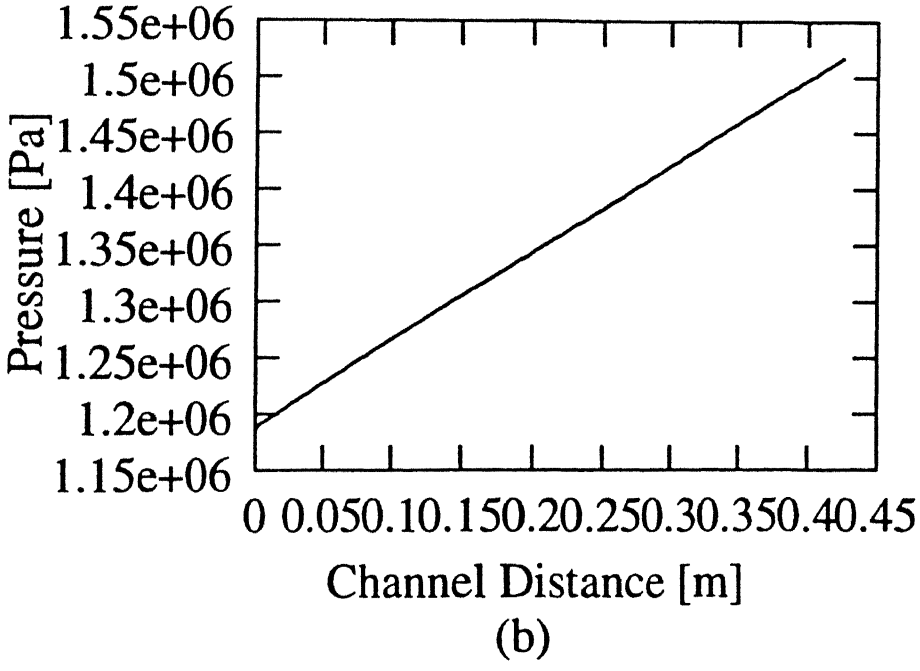

Figure 3.4 Variation of (a)Screw surface temperature and (b)Pressure along the screw channel of a single-screw extruder. Fluid Viscasil, T_b = 80°C, T_i = 53 8°C, q_v = 0 32, N = 60rpm

Chapter 4

COMPARISON OF NUMERICAL RESULTS FOR CORN SYRUP AND LDPE

4.1 The Viscosity Models for Corn Syrup and LDPE

In the present chapter, a Newtonian fluid such as corn syrup is considered. The numerical results are compared with those for a non-Newtonian fluid LDPE (Low Density Polyethylene) for the identical screw configuration and input data in the dimensional form. The viscosity model for corn syrup is given as (Sastrohartono et al., 1995):

$$\mu = 1052.8exp[-0.095(T - 20)] \tag{4.1}$$

where μ is the viscosity in poise, T is the temperature in ^{0}C.

The density, thermal conductivity and the specific heat of corn syrup are :

$$\rho = 1381 \text{ kg } m^{-3}$$

$$K_f = 0.317 \text{ W} m^{-1} K^{-1}.$$

$$C_p = 2015 \text{ J} kg^{-1} K^{-1}.$$

While the Viscosity model (power law) for LDPE is :

$$\mu = \mu_o (\frac{\gamma}{\gamma_o})^{n-1} exp[-b(T - T_o)] \tag{4.2}$$

where μ is the viscosity in Pa-s, T is the temperature in ^oC, and $\dot{\gamma}$ is the shear rate in s^{-1}. The values of constants for the present case are:

$$\mu_o = 2000 \text{ Pa-s.}$$

$$T_o = 200 \text{ °C.}$$

$$b = 0.01 \text{ } ^oC^{-1}.$$

$$\dot{\gamma}_o = 1 \text{ } s^{-1}.$$

power law index $n = 0.48$

and density $\rho = 979$ kg m^{-3}

The thermal conductivity and the specific heat are :

$$K_f = 0.155758 \text{ W} m^{-1} K^{-1}.$$

$$C_p = 1507.16 \text{ J} kg^{-1} K^{-1}.$$

4.2 Screw Configuration and Input Data

The screw elements dimensions are similar to one shown in Table 3.1. The dimensionless parameters (Pe and G) for each case are given in Table 4.1 and Table 4.2. Note the values are different.

The case presented here is for:

barrel temperature $T_b = 80^0$ C

screw speed $N = 60$ RPM.

inlet temperature for the metering section $T_i = 53.8^0$

Table 4.1: Dimensionless quantities involved for Corn Syrup

Peclet number, Pe	3281.265
Griffith number, G	0.9072
Dimensionless throughput, q_v	0.32

Table 4.2 Dimensionless quantities involved for LDPE

Peclet number, Pe	2734.176
Griffith number, G	2.0134
Dimensionless throughput, q_v	0.32

4.3 Results and Discussion

The comparisons of w^* velocity and melt temperature at the various down channel positions are plotted in Fig.4.1 and Fig.4.2 respectively. From the melt temperature plots it is observed that for heavy Corn syrup the melt temperature rise is lower than that for LDPE, which is due to the higher viscous dissipation in LDPE as it has higher viscosity. The w^* velocity plots (Fig.4.2) at the entry and exit of metering section show that at low y^* velocity for corn syrup is lower than that for LDPE while at higher y^* it is just the opposite. This can be explained by the fact that for LDPE viscosity is a function of temperature and shear rate, while for corn syrup it is a function

of temperature only. Near the wall the shear rate is higher than farther away from the wall. Thus for LDPE, viscosity which is a function of negative power of shear rate, is lesser near the wall than farther from it and the velocity w^* of LDPE will be higher there, while corn syrup has no such effect as it is independent of shear rate. Due to heat input at the barrel and viscous dissipation the fluid temperature rises along the length of the channel. This results in decrease in local viscosity and hence the velocity field changes. But the change observed is not much since the temperature difference is small. The screw surface temperature (Fig.4.3(a)) is seen to rise continuously for both cases. It is interesting to note little difference between the two. One reason may be the almost identical thermal conductivity ratio (K_s/K_f) for LDPE and corn syrup, as for both cases the same screw material is taken and K_f for both are almost the same. The slightly higher screw surface temperature for corn syrup in about first 66% length of the channel may be due to the fact that because of higher cross thermal convection for corn syrup (large Peclet number) the barrel heat is convected better to the screw surface and hence the screw surface temperature is greater. However, towards the exit the screw surface temperature for the corn syrup is lower because of greater viscous dissipation effect for LDPE as it has higher apparent viscosity (Griffith number for LDPE is greater). Also, it is noted that the screw surface temperature for both the cases approaches the barrel temperature, due to the combined effects of cross thermal convection and viscous heat dissipation. The pressure is seen to rise continuously for both cases (Fig.4.3(b)). But the rise is higher for LDPE than for corn syrup, again due to higher viscosity of LDPE.

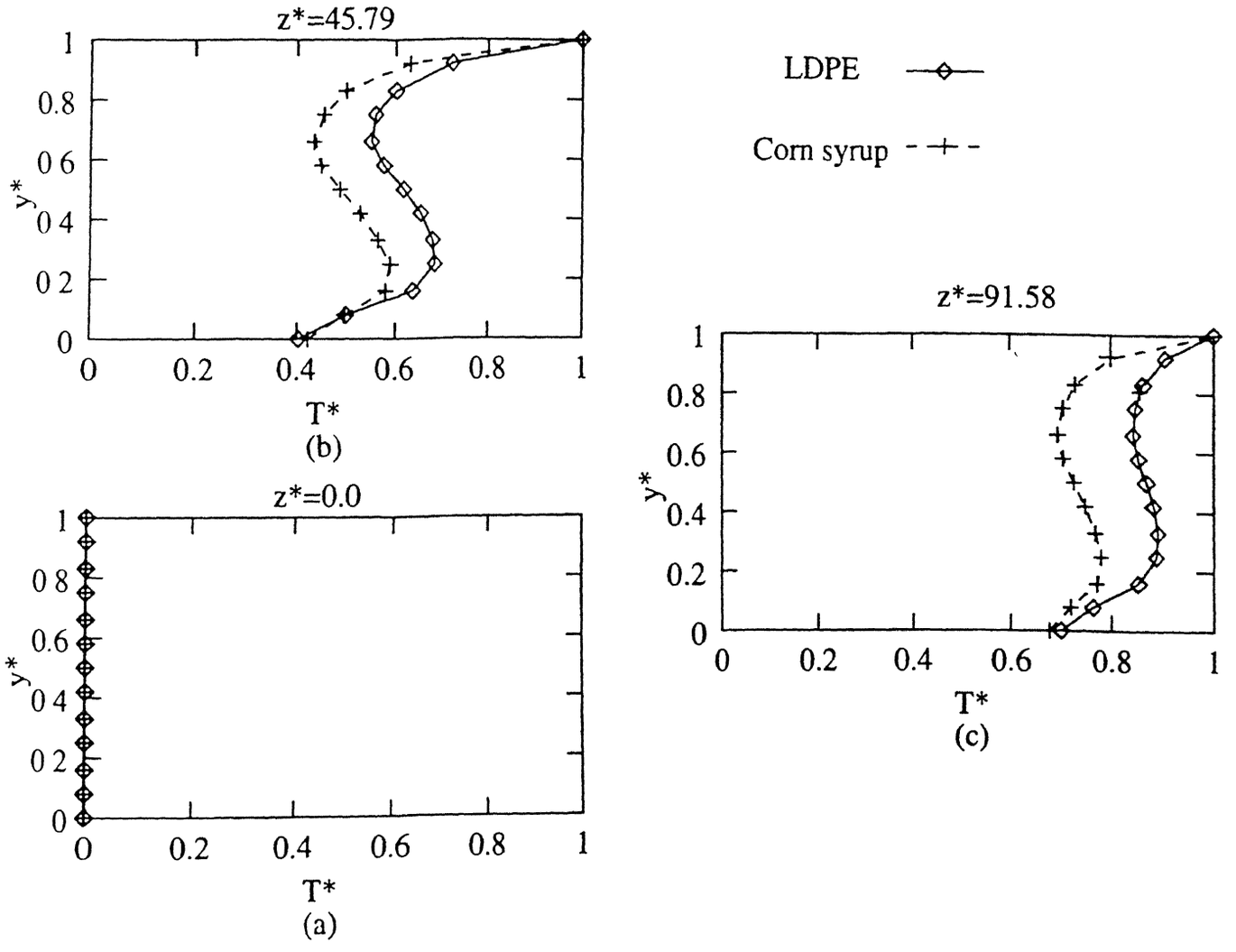

Figure 4.1 Comparison of melt temperature profiles along the screw channel for various z locations

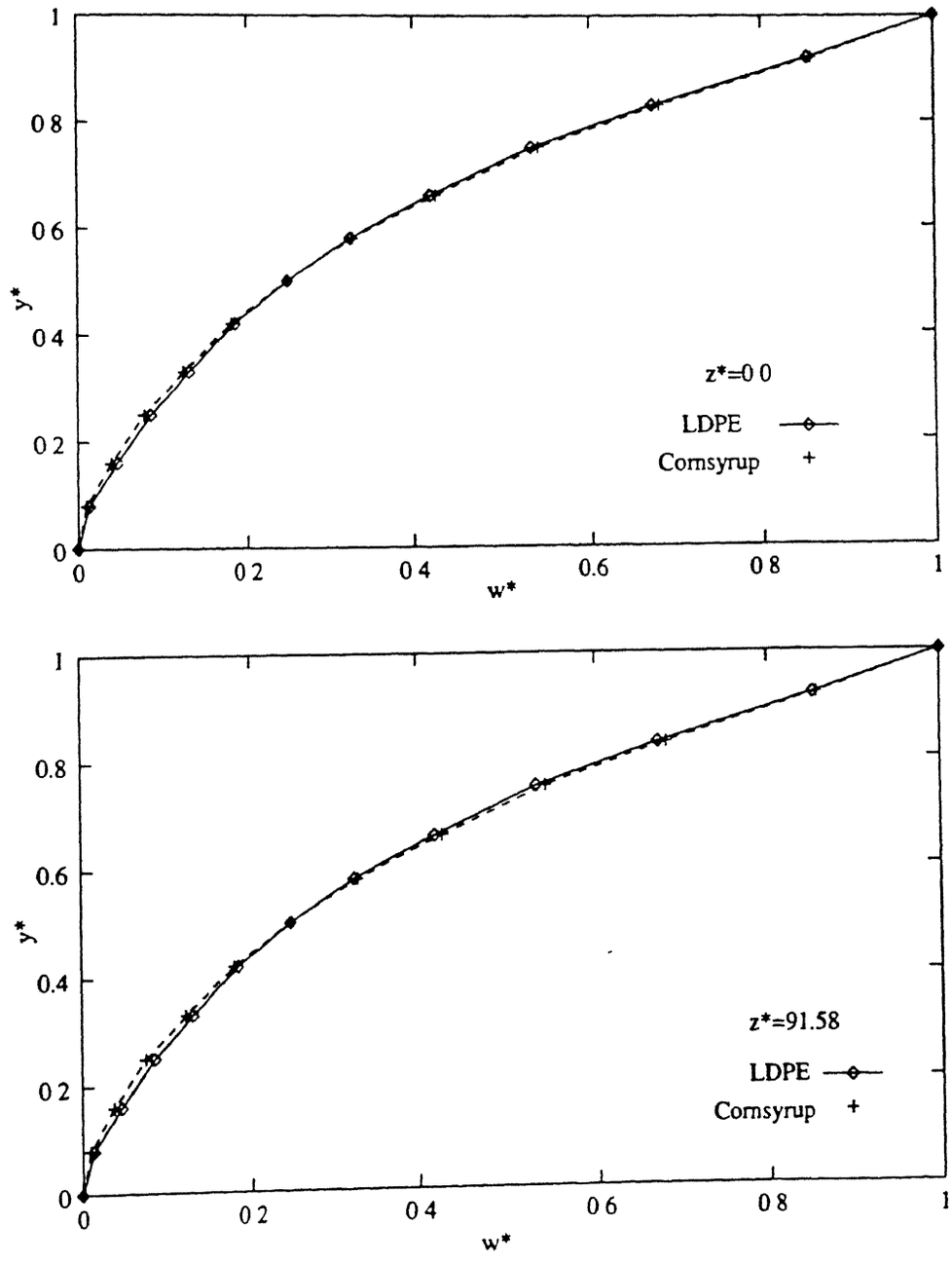

Figure 4 2 Comparison of w^* velocity profiles along the screw channel for various z locations

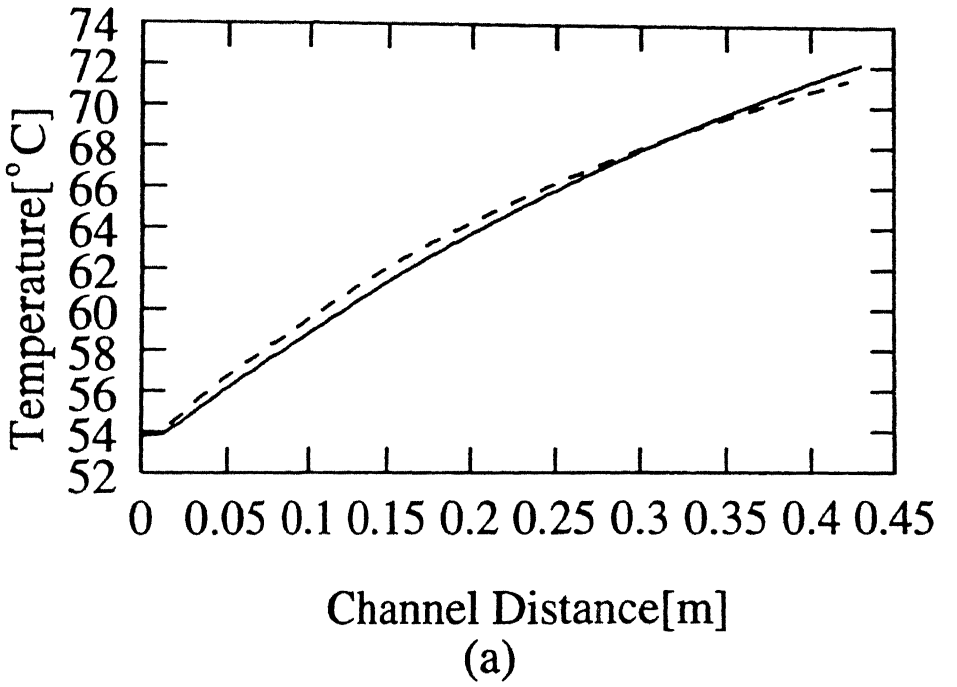

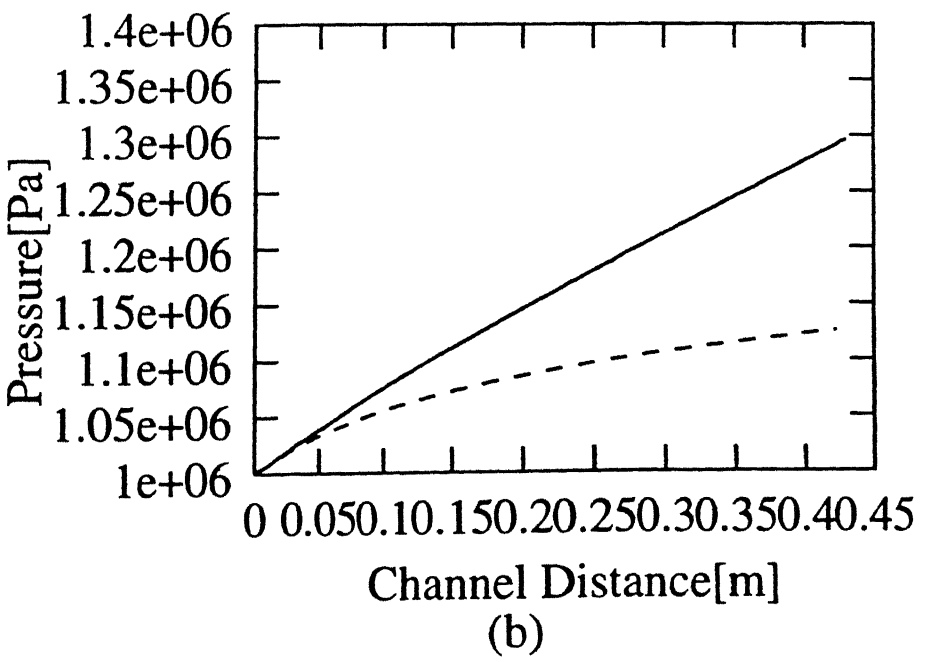

Cornsyrup - - - -

LDPE ———

Figure 4 3: Comparison of (a) Screw surface temperature and (b) Pressure along the screw channel between LDPE and corn syrup

Chapter 5

NUMERICAL RESULTS FOR DEFATTED SOY FLOUR PROCESSING AND ITS VALIDATION WITH EXPERIMENTAL RESULTS OF FONG(1978)

5.1 Viscosity Model used for Defatted Soy Flour Dough

In this chapter defatted soy flour is considered and a comparison of the results is done with the experimental results obtained by Fong (1978).

The viscosity model used for defatted soy flour is power law model, given as follows:

$$\mu = \mu_o(\frac{\dot{\gamma}}{\gamma_o})^{n-1} exp[-b(T - T_o)] \tag{5.1}$$

where μ is the viscosity in Pa-s, T is the temperature in °C, and $\dot{\gamma}$ is the shear rate in s^{-1}.

The power-law index, n and constant, μ_o calculated from the experimental results obtained by Fong (1978) are listed in Table 5.1 for three moisture contents. The method used for computation is given in Appendix A.

Table 5 1: The value of μ_o and n for three moisture contents

Dough flour moisture [% by weight]	33%	28%	25%
μ_o [Pa-s]	32763.0	123010.0	134215.0
n	0.4569	0.1222	0.0177

For each case, the value of b and $\dot{\gamma}_o$ are $0.01°C^{-1}$ and $1s^{-1}$ respectively.

5.2 Screw Configuration and Input Data

The results presented here for quasi 3-D model are compared with the experimental results obtained by Fong (1978). The screw configuration and input

data are given in Table 5.2. While the dimensionless parameters in three cases are given in Tables 5.3, 5.4 and 5.5. It may be noted that in absence of reliable information regarding 'b' for soy flour , the corresponding value for LDPE has been used. Similarly, the thermal conductivity, K_f for soy flour dough was not available and hence K_f for wheat flour (Singh, 1978) was used. It is expected that aforementioned uncertainties in input data will not seriously effect the results as for the soy flour processing 'melting' model is used and conductivity of wheat flour should be close to that of soy flour.

Table 5 2 Screw configuration and input data

Screw Diameter, D	25.4 mm.
Helix angle, ϕ	17.5^o
Maximum channel depth, H	1.46 mm.
Maximum channel width, W	19.3 mm.
Length of metering section, L_m	167.64 mm.
Density, ρ	1220 Kg m^{-3}
Thermal Conductivity (dough), K_f	0.45 $Wm^{-1}K^{-1}$.
Thermal Conductivity (screw), K_s	45 $Wm^{-1}K^{-1}$.
Specific Heat, C_p	3320 $JKg^{-1}K^{-1}$.
Barrel temperature T_b	73.89^0 C
Screw speed N	26 RPM.
Inlet temperature for the metering section T_i	62.7^0 C

Table 5.3· Dimensionless parameters involved for 33% moisture content Soy flour dough

Peclet number, Pe	396.260
Griffith number, G	1.588
Dimensionless throughput, q_v	0.0942

Table 5 4 Dimensionless parameters involved for 28% moisture content Soy flour dough

Peclet number, Pe	396.260
Griffith number, G	2.0393
Dimensionless throughput, q_v	0.1847

Table 5 5 Dimensionless parameters involved for 25% moisture content Soy flour dough

Peclet number, Pe	396.260
Griffith number, G	1.5915
Dimensionless throughput, q_v	0.1955

5.3 Results and Discussion

The velocity vector plots for 25% moisture content dough (Fig. 5.1) show weak recirculation in the cross-sectional plane which is due to the high viscosity of low moisture dough. A high recirculation is seen for 28% and 33% moisture content dough (Fig. 5.5 and Fig .5.9 respectively) since viscosity is comparatively lower in this case due to high moisture presence which facilitates the motion. The down channel velocity w^* variation with y^* at various z locations shows that back flow occurs. This was also reported by Fong (1978). The backflows for 25%(Fig. 5 2) case and 28% (Fig. 5.6) case are small while for the case of 33% moisture backflow is larger. This is due to the difference in normalised flow rate q_v of the three cases (see Table 5.3,5.4 and 5.5). Since a smaller q_v implies that the die opening is small, thus not all dough can pass through it and some of it flows in the backward direction.

For the temperature profile at various z locations, it is noticed that temperature is always higher than the barrel temperature. This was also reported during the experiments by Fong (1978). Also temperature rise is higher in the case of 25% dough (Fig. 5.3) than other two cases (Fig. 5.7 and Fig. 5.11).

This is due to higher moisture contents and hence lesser viscous dissipation in the latter cases.

The pressure is seen to rise linearly for all three cases viz. 25% (Fig 5.4(b)), 28% (Fig. 5.8(b)) and 33% (Fig. 5.12(b)). Though pressure rise is more in the case of 25% moisture than 28% case, which in turn is more than the 33% case due to higher viscosity for the former cases. The screw surface temperature rises very rapidly in the early part of the metering section and then steadies to a temperature much greater than the barrel temperature (Fig. 5.4(a), Fig. 5.8(a) and Fig. 5.12(a)). This is due to very high viscous heat dissipation in food as compared to polymer

5.4 Experimental Validation

Table 5.6 shows computed and experimental outlet bulk temperatures for all three cases. It is seen that for low moisture percentages the difference in temperature is much higher than that at high moisture percentage. A similar trend is observed in the case of outlet pressure (comparisons shown in Table 5.7).

This can be explained due to the fact that at lower moisture percentage viscosity is high and hence more heating takes place which initiates cooking reaction. This cooking reaction changes the viscosity which can not be simply represented by the power law model. But for high moisture percentage case a better agreement between two results is seen i.e. cooking here has less effect on the viscosity of the fluid . So this model is inadequate for high temperature and low moisture case but can be effectively used for low temperature and high moisture case.

Table 5.6 Comparison of computed and experimental outlet temperature

Moisture percentage	Outlet Temperature (Experimental) [°C]	Outlet Temperature (Computed) [^{o}C]
25	110.46	93.998
28	100.10	91.422
33	81.70	80.64

Table 5 7 Comparison of computed and experimental outlet pressure

Moisture percentage	Outlet Pressure (Experimental) [x 10^{6} Nm^{-2}]	Outlet Pressure (Computed) [x $10^{6}Nm^{-2}$]
25	5.040	2.76
28	4.912	2.67
33	1.480	1.34

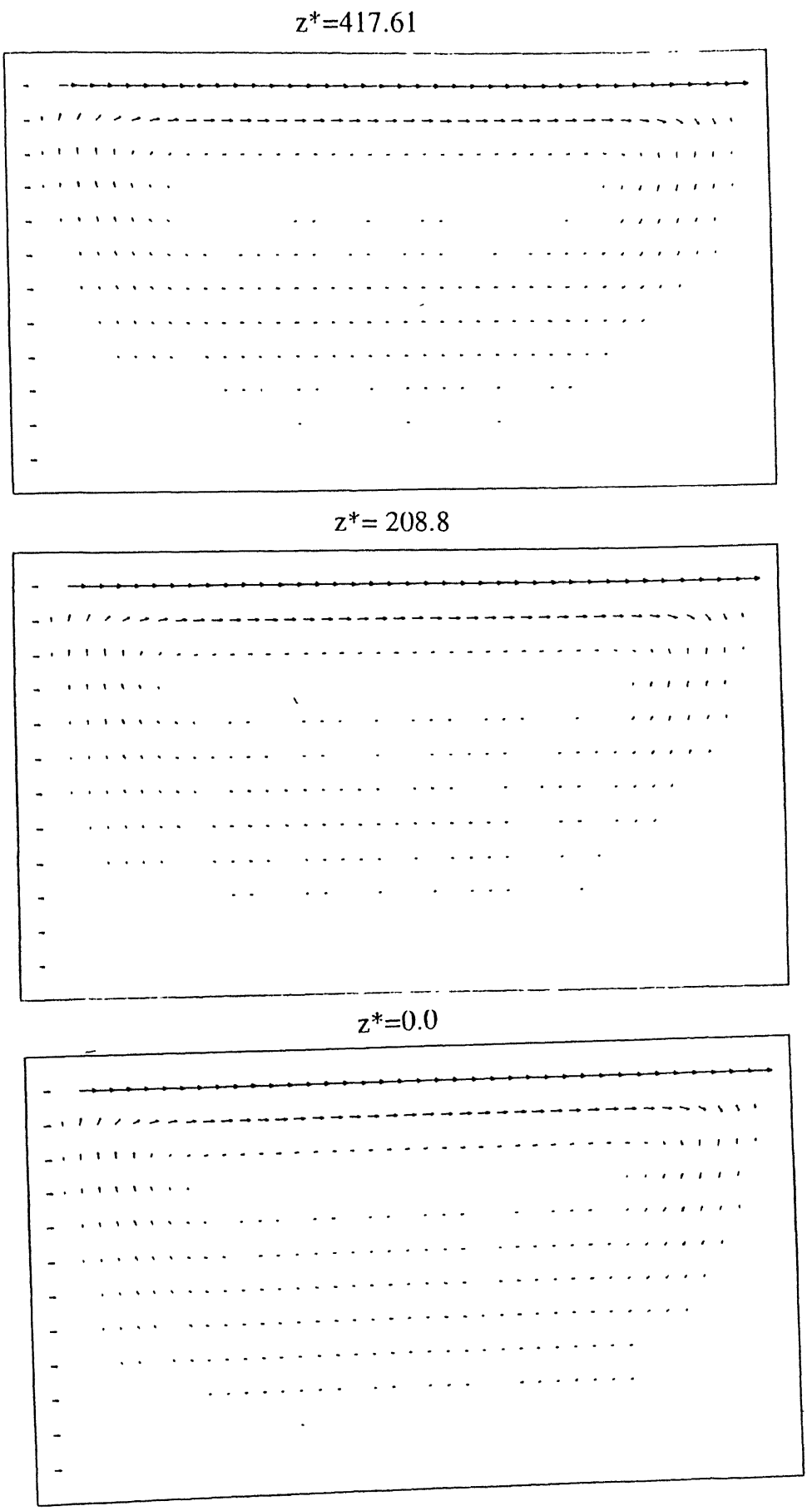

Figure 5 1· Velocity vector plots for 25% moisture content dough at three down channel locations

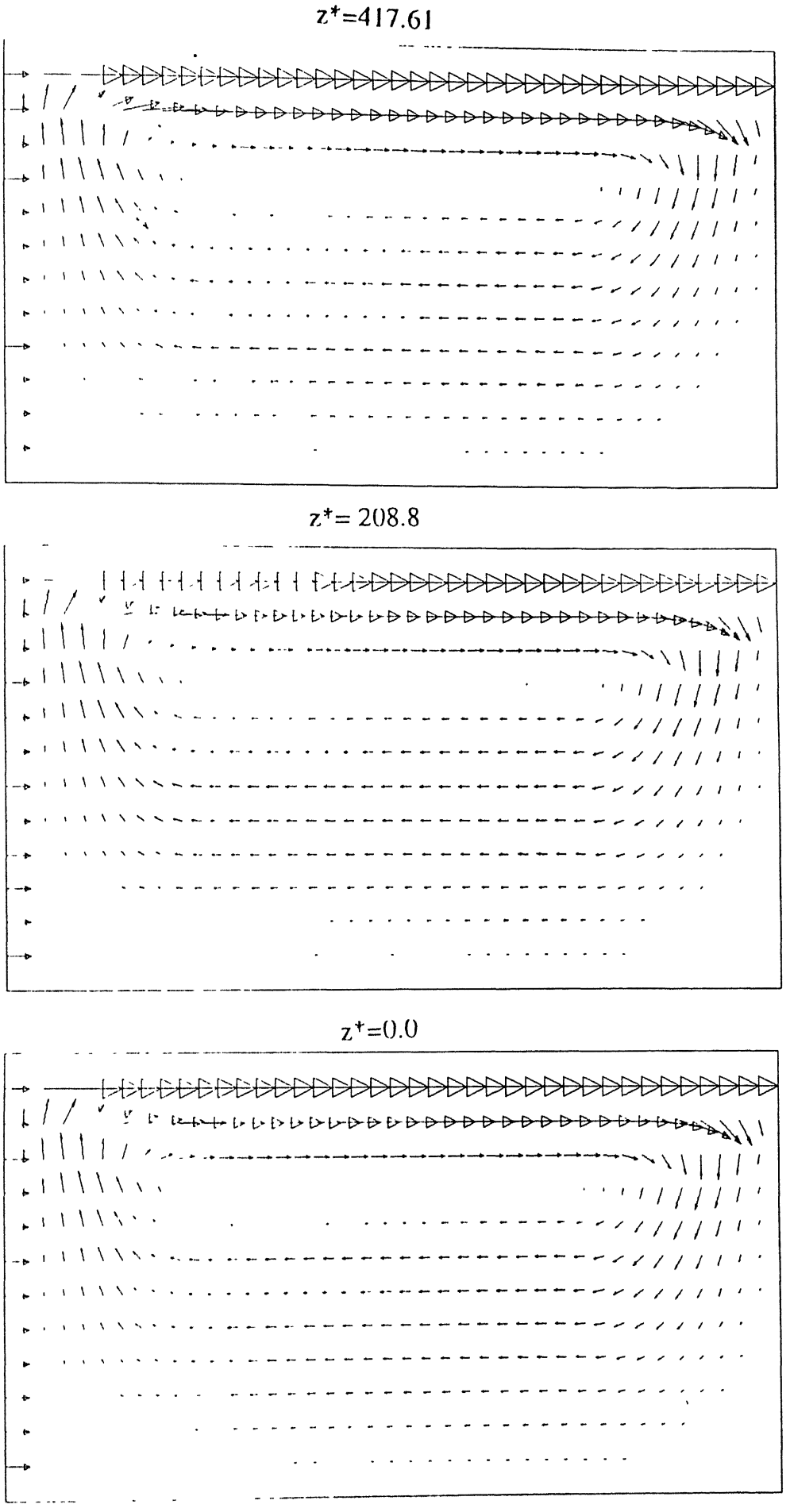

Figure 5 1 Velocity vector plots for 25% moisture content dough at three down channel locations

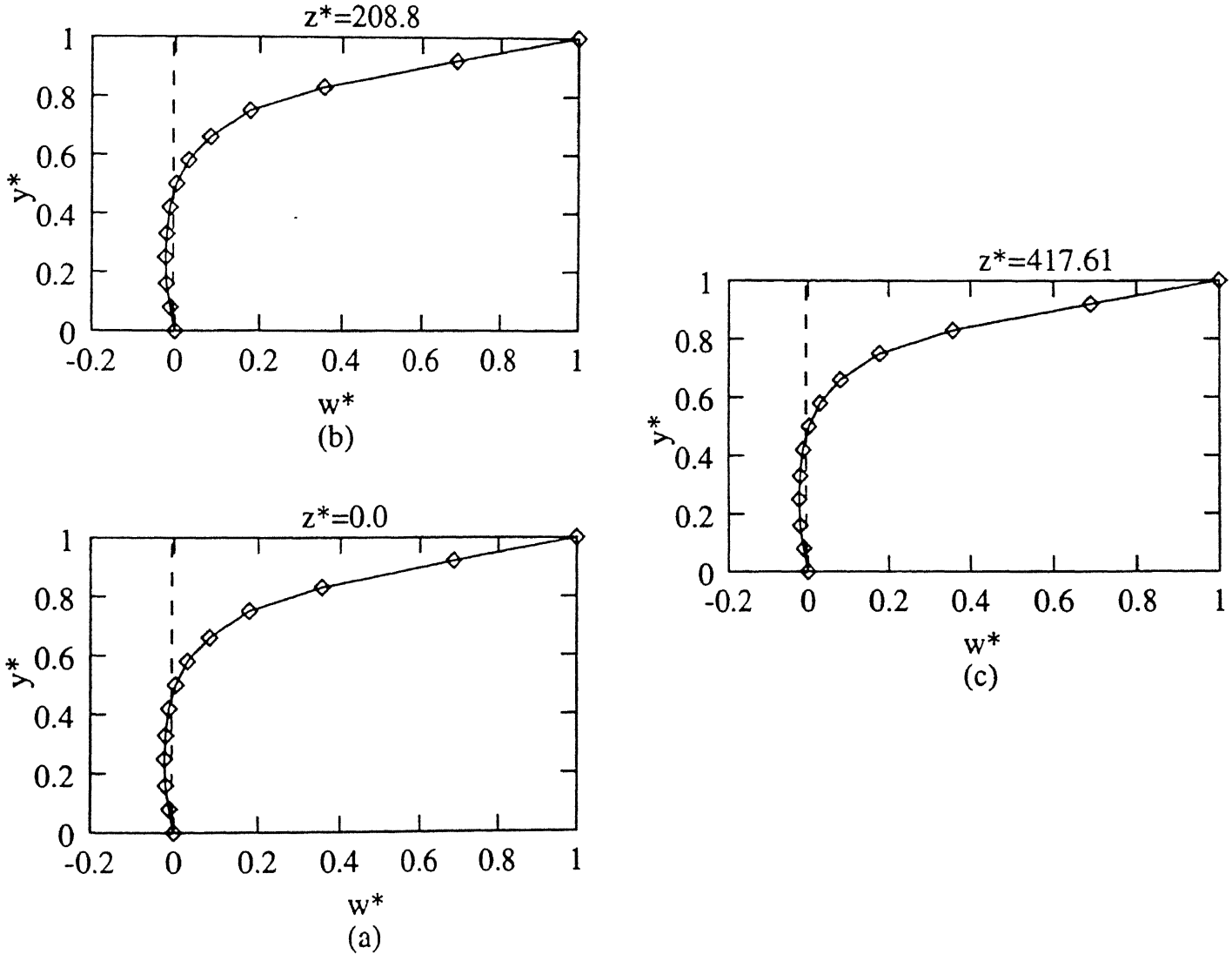

Figure 5.2 w^* velocity profiles for 25% moisture content dough at three down channel locations

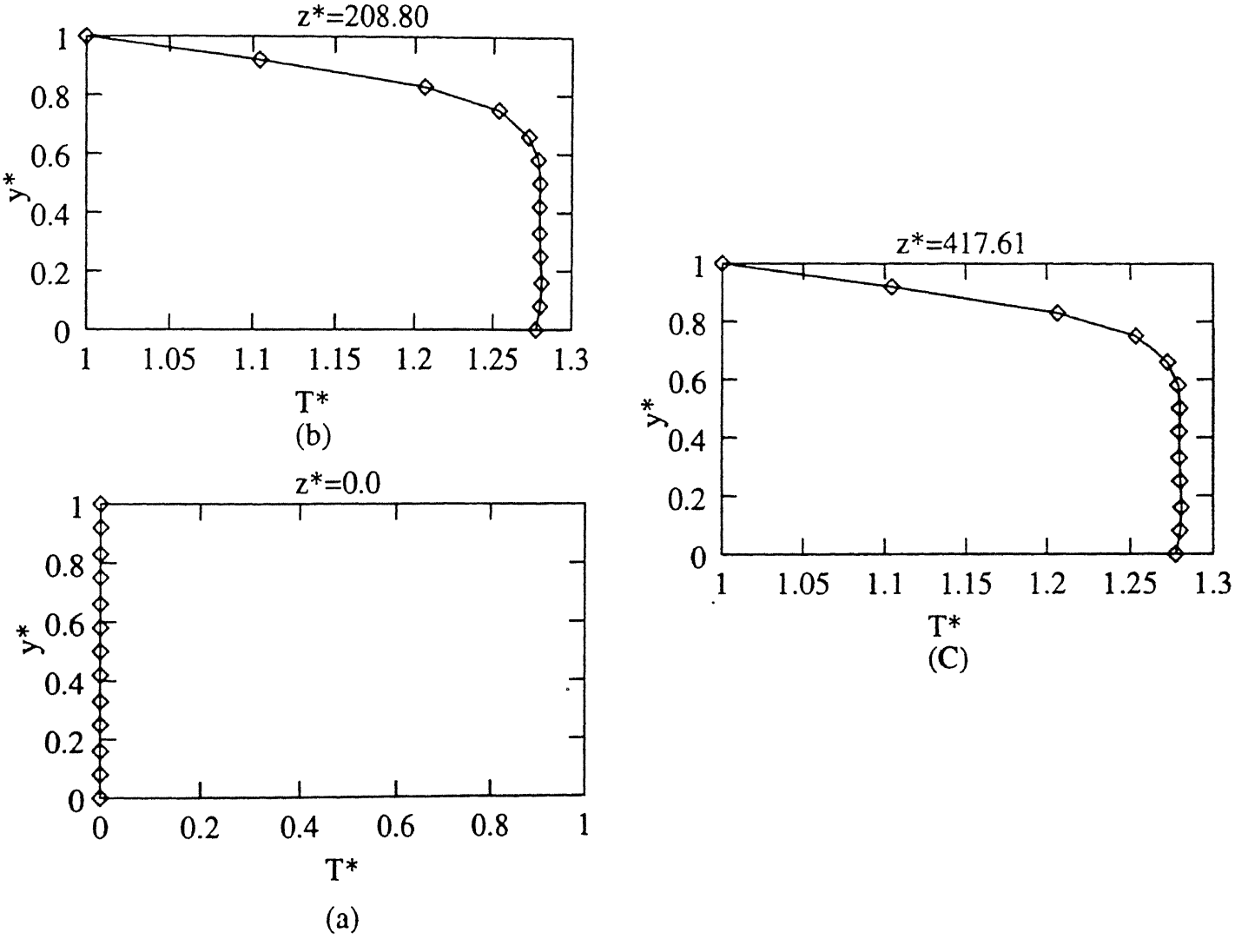

Figure 5.3 Temperature profiles for 25% moisture content dough at three down channel locations

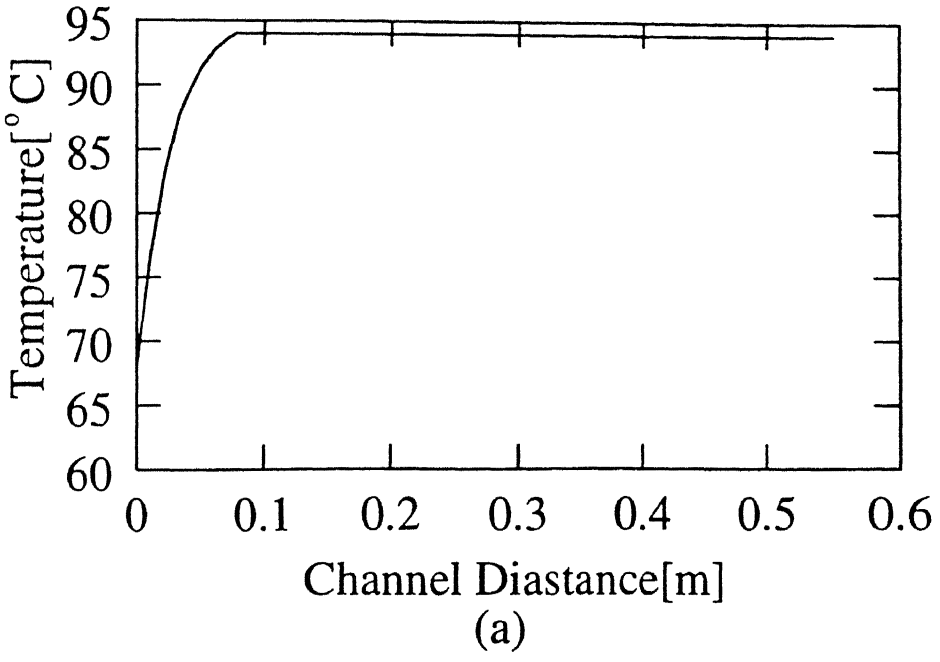

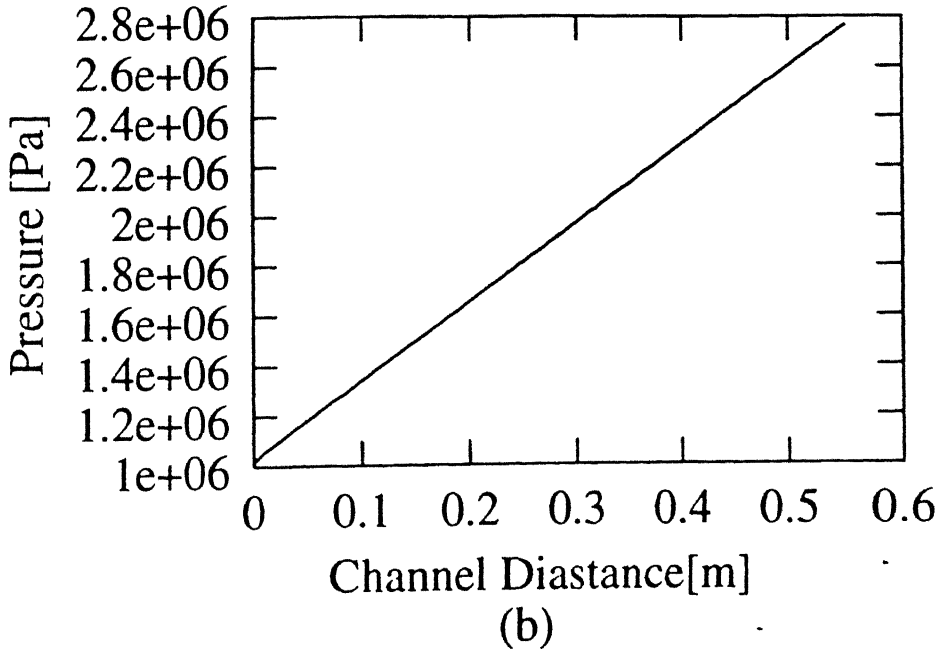

Figure 5.4 (a)Screw surface temperature and (b)Pressure variation along the length of screw extruder for 25% moisture content dough

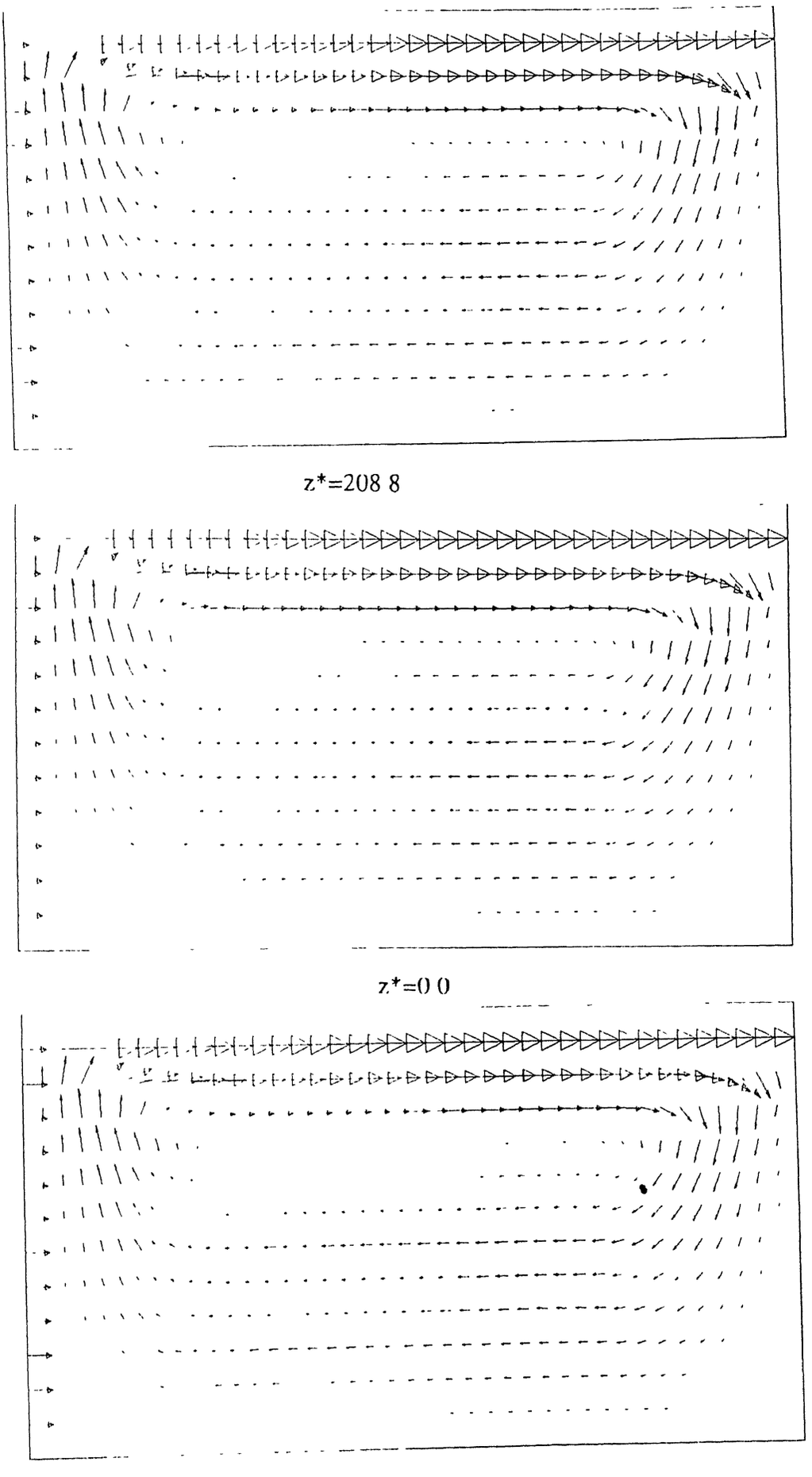

Figure 5 5 Velocity vector plots for 28% moisture content dough at three down channel locations

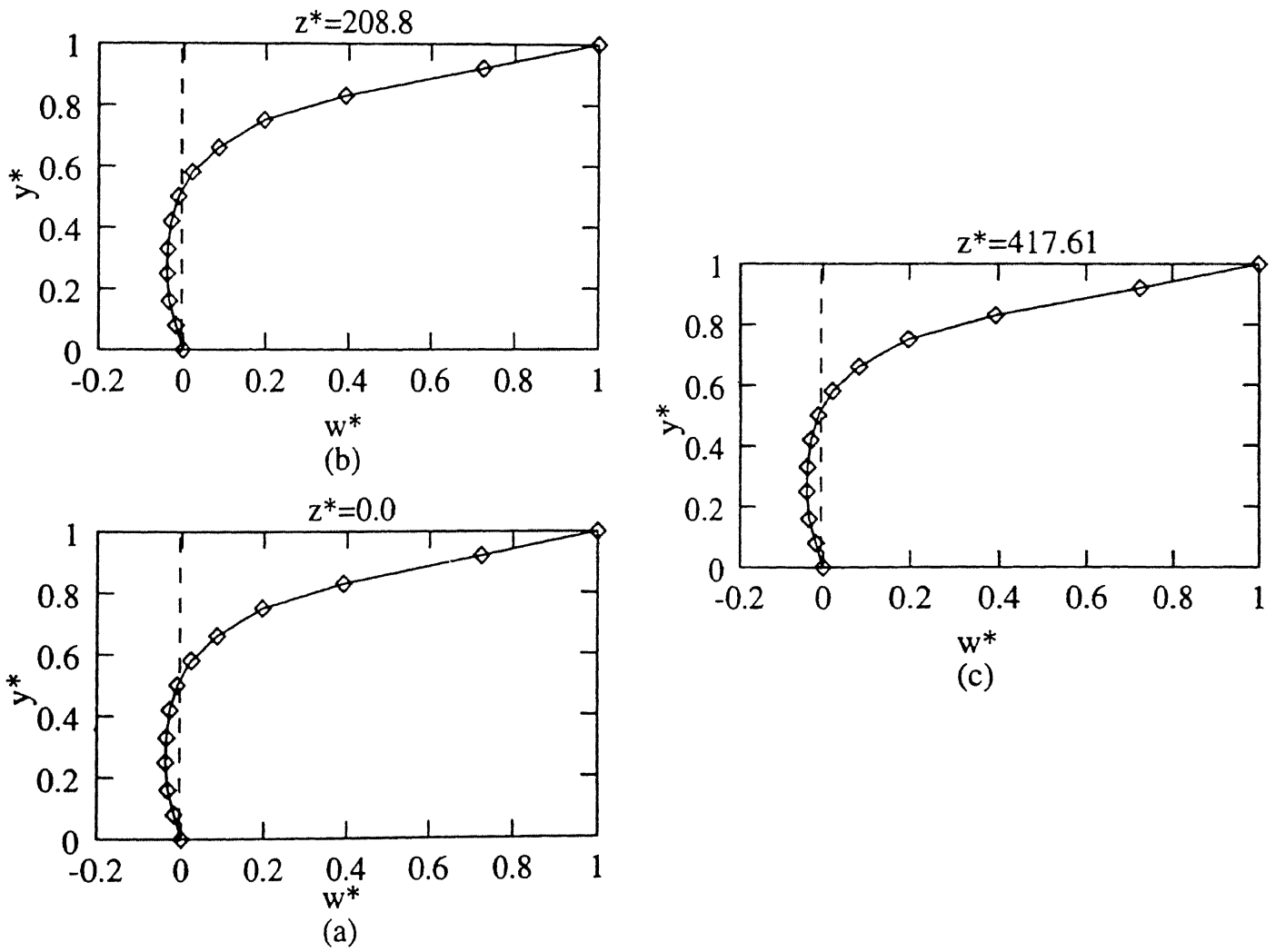

Figure 5 6 w^* velocity profiles for 28% moisture content dough at three down channel locations

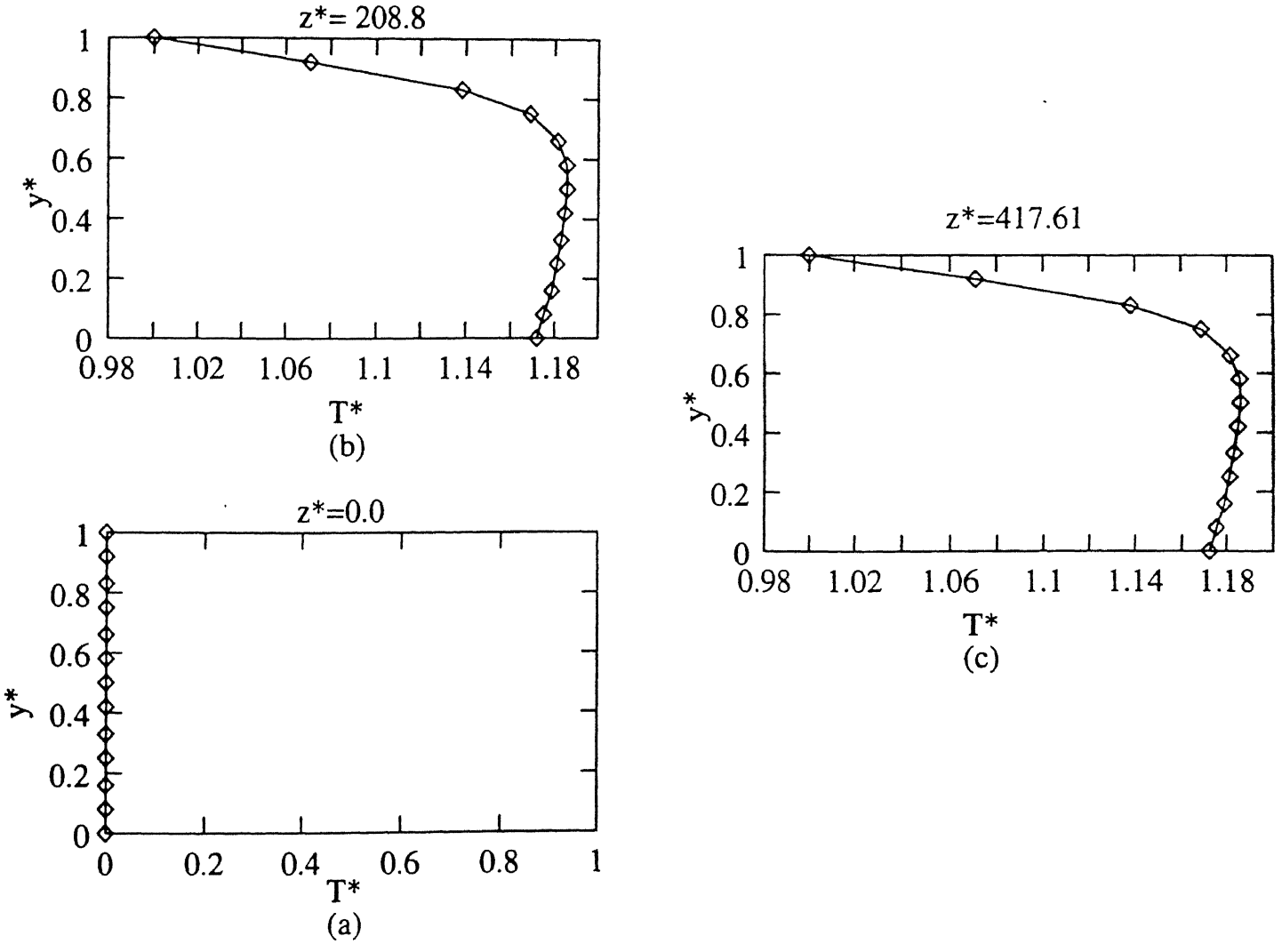

Figure 5 7 Temperature profiles for 28% moisture content dough at three down channel locations

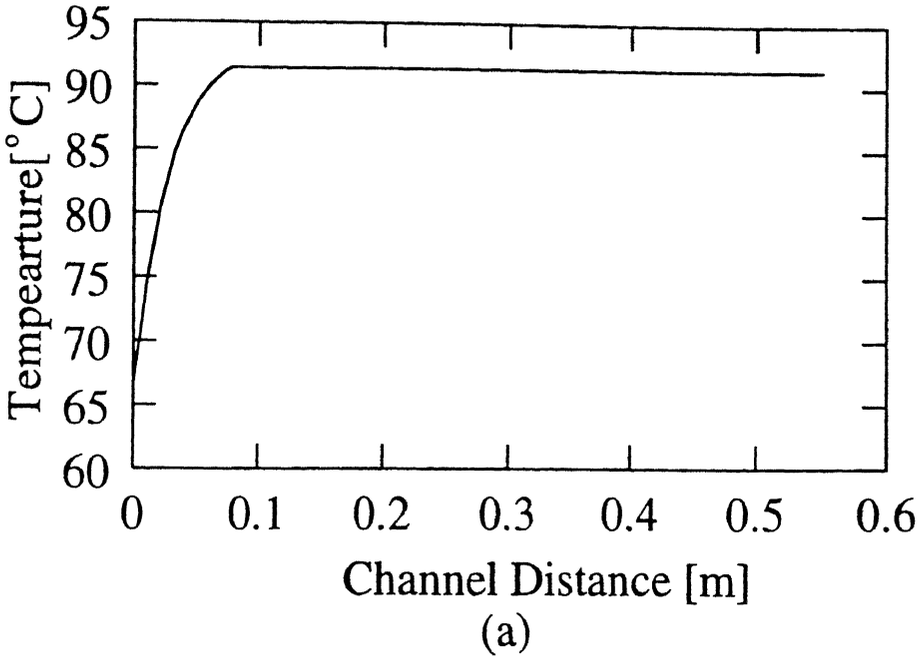

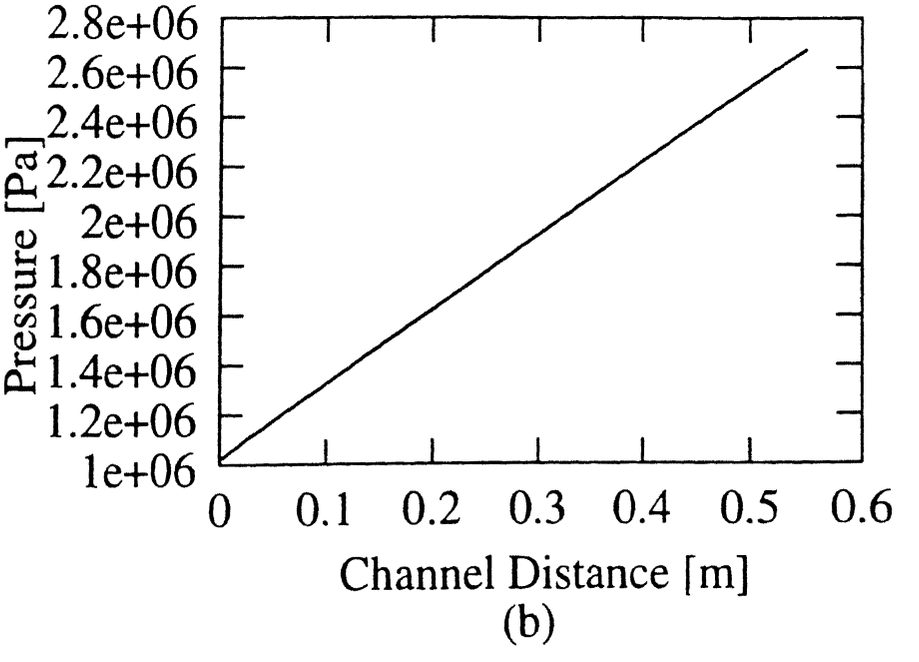

Figure 5 8 (a)Screw surface temperature and (b)Pressure variation along the length of screw extruder for 28% moisture content dough

z*=417.61

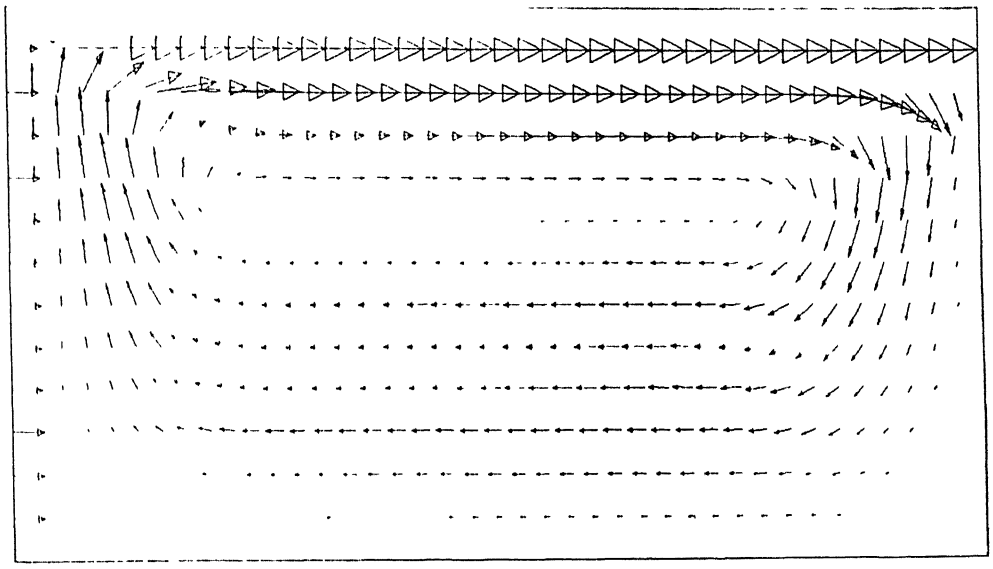

z*=208.8

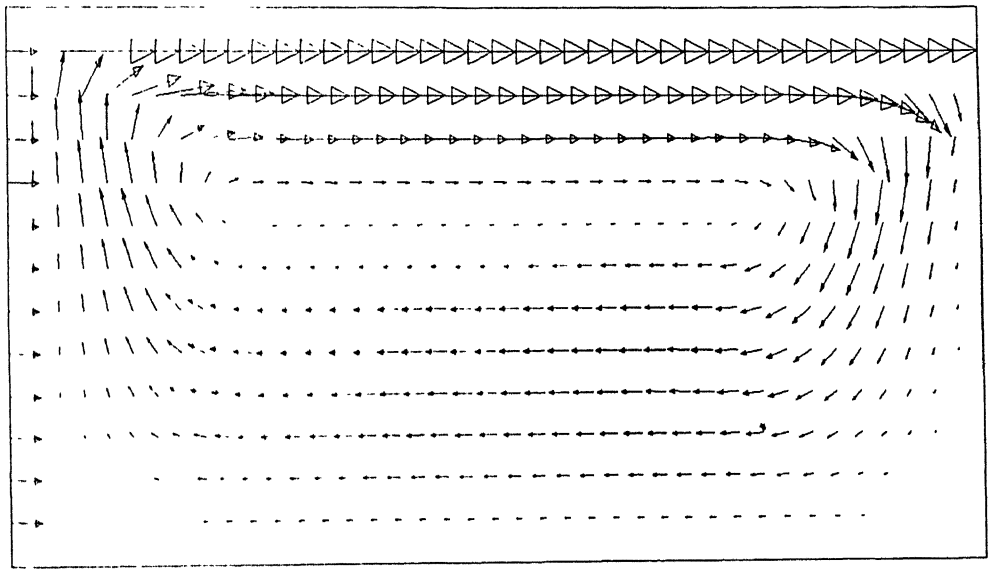

z*=0.0

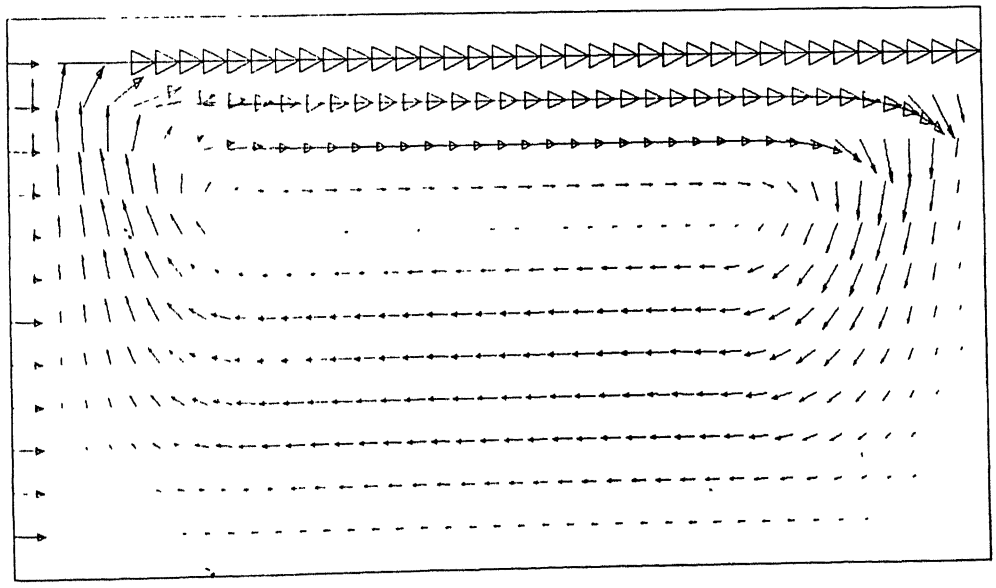

Figure 5.9: Velocity vector plots for 33% moisture content dough at three down channel locations

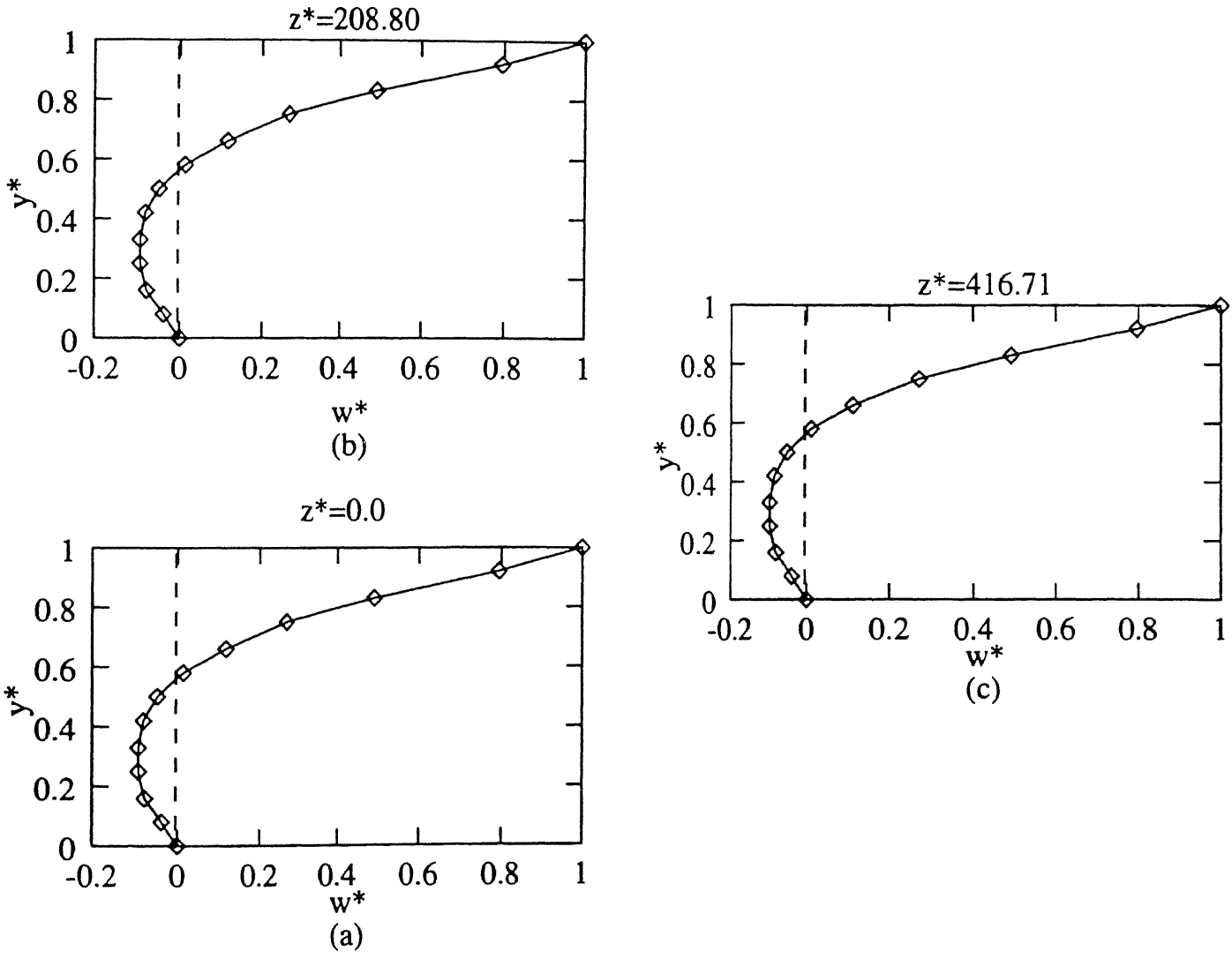

Figure 5.10 w^* velocity profiles for 33% moisture content dough at three down channel locations

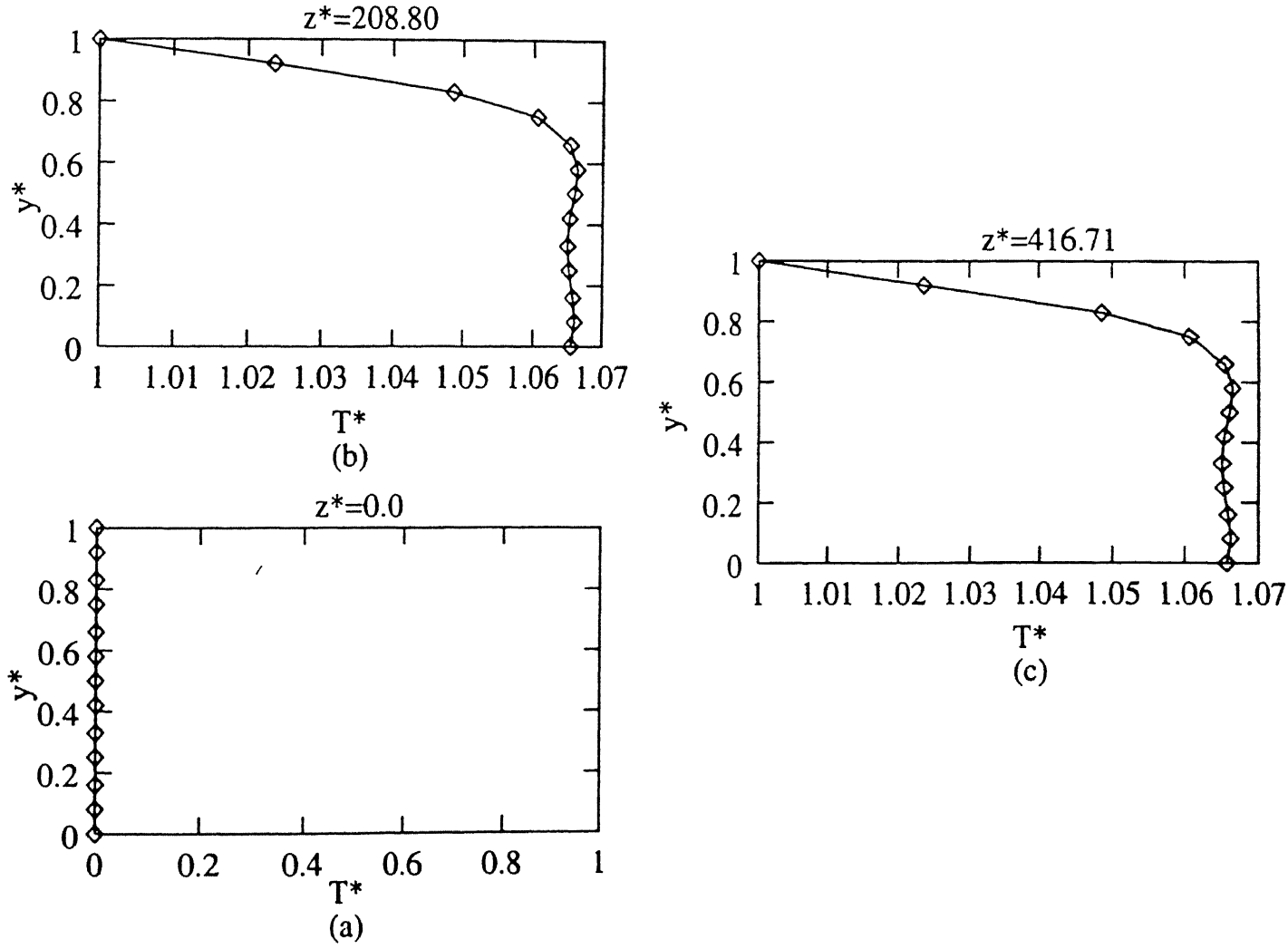

Figure 5 11 Temperature profiles for 33% moisture content dough at three down channel locations

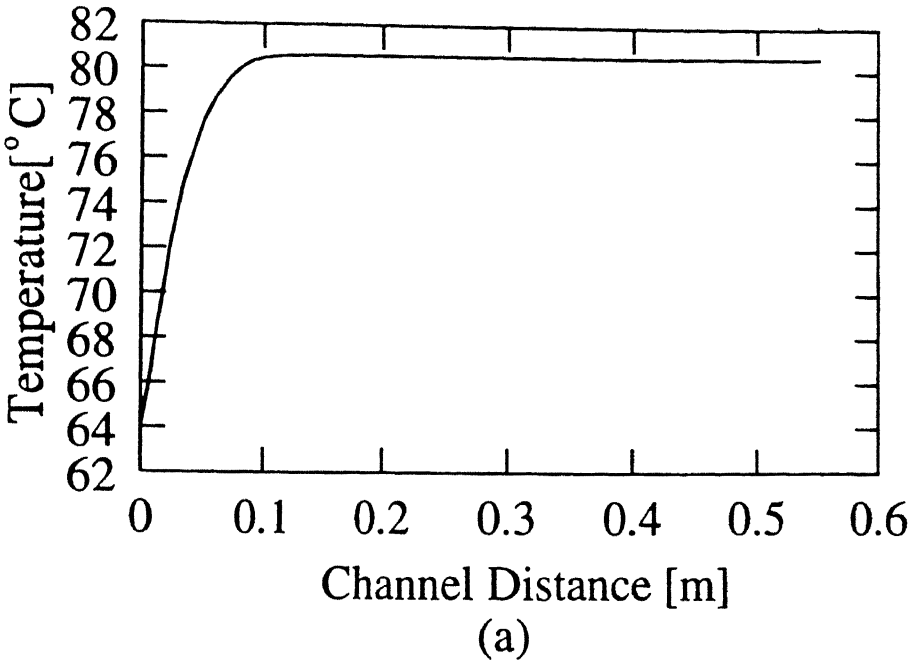

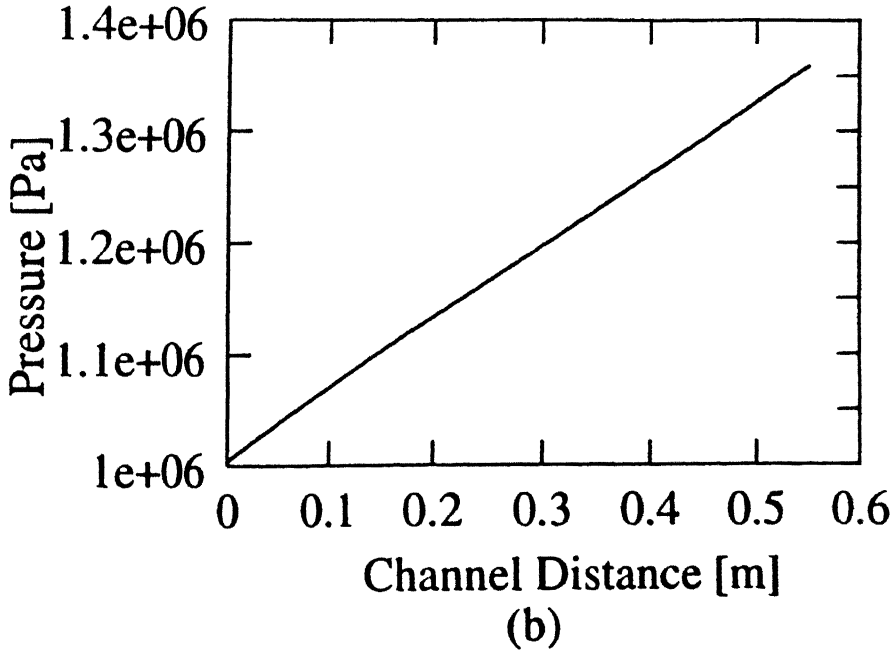

Figure 5.12: (a)Screw surface temperature and (b)Pressure variation along the length of screw extruder for 33% moisture content dough

Chapter 6

CONCLUSIONS AND SCOPE FOR FUTURE WORK

6.1 Conclusions

A numerical study of 3-D flow and heat transfer during processing of polymers and foods in the metering section of a single screw extruder is carried out. A quasi 3-D finite volume modelling is used and flow field in cross-sectional plane is calculated using SIMPLE algorithm. A fully implicit scheme is used to march along the length of the channel. The computer model is capable of predicting the flow even for very small die opening (very low q_v cases) which gives rise to back flow situations, as in processing of food doughs.

The polymers considered are LDPE and Viscasil, while the foods are heavy corn syrup and defatted soy flour. One of the achievements of this work is to successfully extend the quasi 3-D model of Das and Ghoshdastidar (1994b) for power-law fluids to non-power law fluids like Viscasil. This has also been validated by comparison with experimental results of Sastrohartono et al.

(c) To find that power-law viscosity model ("melting" model) is reliable for high moisture content defatted soy flour dough but not so for drier doughs. It may also be noted that for the first time a quasi 3-D model using power-law viscosity model has been used to simulate food dough processing.

6.2 Scope for Future Work

For the purpose of initial application, the results have been shown for only one dough material (i.e. defatted soy flour) with only three levels of moisture content. Once a good viscosity model for all levels of moisture contents is developed, it is desirable to extend the applications to other food materials such as corn, wheat, rice etc.

Appendix A

PROCEDURE FOR COMPUTATION OF CONSTANTS OF POWER LAW MODEL

A.1 Procedure for Calculation of μ_o and n

Here a calculation procedure proposed by Rogers (1970) is presented to estimate μ_o and n, the constants of power law equation for describing the viscosity behaviour of defatted soy flour. The use of procedure requires pressure drop and flow data using a number of dies having varying L/R ratios.

The viscosity model used for deffated soy flour is power law model, given as follows:

$$\mu = \mu_o(\frac{\dot{\gamma}}{\gamma_o})^{n-1} exp[-b(T - T_o)] \qquad (A.1)$$

where μ is the viscosity in Pa-s, T is the temperature in °C, and $\dot{\gamma}$ is the shear rate in s^{-1}.

The experimental data used here for calculation is taken from Fong (1978). The dimension of dies used by him for extrusion were:

Table A 1. Dimensions of Die

Die	D [mm]	L [mm]
1	10.16	49.53
2	11.43	55.88

The data taken for dough is tabulated in Table A.2 and Table A.3 for die 1 and die 2 respectively.

Table A 2: Mass flow rate and exit pressure values for the Die 1

Reading	Mass flow rate [gm/min]	Volume flow rate Q [x $10^{-8}m^3$/s]	Exit Pressure ΔP [x 10^6 Pa]
1	7.1	9.47	1.48
2	13.8	18.10	2.09
3	21.4	20.08	2.55

Table A 3 Mass flow rate and exit pressure values for the Die 2

Reading	Mass flow rate [gm/min]	Volume flow rate Q [x $10^{-8}m^3/s$]	Exit Pressure ΔP [x 10^6 Pa]
1	9.5	12.97	1.02
2	13.4	18.30	1.50
3	20.5	28.00	2.08

For the solution from the data we calculate $\dot{\gamma}_a$ given as:

$$\dot{\gamma}_a = \frac{4Q}{\pi R^3} \tag{A.2}$$

The calculated values are given in Table A.4.Then $\log\dot{\gamma}_a$ vs. $\log p$ is plotted and from the graph ΔP is found for $\dot{\gamma}_a = 1s^{-1}$ and $2s^{-1}$ for each die. These values are given in table A.5 along with L/R values of both the dies.

Table A.4 Value of $\dot{\gamma}_a$ for Die 1 and Die 2

Reading	Die 1 $\dot{\gamma}_a[s^{-1}]$	Die 2 $\dot{\gamma}_a[s^{-1}]$
1	0.9194	0.8845
2	1.7579	1.2483
3	2.7275	1.910

Table A 5 Value of ΔP for $\dot{\gamma}_a$ $1s^{-1}$ and $2s^{-1}$ for Die 1 and Die 2

$\dot{\gamma}_a$ $[s^{-1}]$	$log\Delta$P L/R = 9.75	$log\Delta$P L/R = 9.78
1	14.2556	13.9728
2	14.6031	14.6104

Now ΔP vs. L/R is plotted and then extrapolated to obtain L^*/R, which is the value corresponding to ΔP = 0 (given in Table A.6).

Table A 6· L^*/R value for γ_a $1s^{-1}$ and $2s^{-1}$

$\dot{\gamma}_a$ $[s^{-1}]$	L^*/R
1	8.5192
2	9.0925

These L^*/R values are plotted against $\dot{\gamma}_a$ to get their values at data points. These values are given in Table A.7.

The values so obtained are used to calculate τ_w, which is given as:

$$\tau_w = \frac{\Delta P}{[2(\frac{L}{R} + \frac{L^*}{R})]} \tag{A.3}$$

These values are given in Table A.8.

Slope of $\log \tau_w$ vs $\log \dot{\gamma}_a$ gives the flow behaviour index. This is found out to be n = 0.4569 in this case. For calculation of μ_o we get $\dot{\gamma}_w$ = (3n+1)(4n)$\dot{\gamma}_a$ and which is used to get $\mu = \tau_w/\dot{\gamma}_w$ (given in Table A.9.

Table A 7· L^*/R value for data points for Die 1 and Die 2

Reading	L^*/R Die 1	L^*/R Die 2
1	8.4497	8.4176
2	8.9858	8.7026
3	9.3490	9.0544

Table A 8 τ_w value for data points for Die 1 and Die 2

Reading	τ_w [x10^4 Pa] Die 1	τ_w [x10^4 Pa] Die 2
1	4.0669	2.8000
2	5.5771	4.0660
3	6.6659	5.5186

The intercept of $\log \mu$ vs. $\log \dot{\gamma}$ gives the value of μ_o. In the present calculation μ_o = 3.2763 x 10^4 Pa.

Table A.9 γ_w value for data points for Die 1 and Die 2

Reading	μ[x 10^4 Pas] Die 1	μ[x 10^4 Pas] Die 2
1	3.4099	0.9160
2	2.2803	1.2928
3	3.5381	1.9781

References

[1] Agur, E.E. and Vlachopoulos, J. 1982, "Numerical Simulation of Single-screw Plasticating Extruder", *Polymer Eng. and Sci.*, Vol.22, No 17, pp 1084-1094.

[2] Bigg, D.M. and Middleman, S , 1974 "Mixing in a Screw Extruder, Model for Residence Time Distribution and Strain", *Ind. Eng. Chem. Fundam.*, Vol.13, pp.66-71

[3] Carnahan, Bruce, Luther, H.A., Wilkes, J.O., 1969, *Applied Numerical Methods*, John Wiley and Sons, New York.

[4] Chen, A.H., Jao, Y.C , Larkin, J.W., Goldstein, W.E., 1978, "Rheological Model of Soy Dough in Extrusion", *J. Food Proc. Engr.*, Vol.2, pp.337-342.

[5] Crevone, N.W. and Harper, J.M., 1978, " Viscosity of an Intermediate moisture Dough",*Presented at 84th AIChE National Meeting,* Atlanta.

[6] Das, Manab K., 1993, *A Detailed Numerical study of Thermal Transport Processes in the Metering section of a Single-screw Plasticating Extruder*, Ph.D. Thesis, Mechanical Engineering, IIT Kanpur.

[7] Das, Manab K. and Ghoshdastidar, P.S., 1994a, "Quasi Two-Dimensional and Fully Two-Dimensional Computer models of Flow

and Conjugate Heat Transfer in the Metering section of a Single-screw Plasticating Extruder. A Comparative Study." *Proc. 10th International Heat Transfer Conference Brighton U.K., August 14-18*, Vol.2, pp.331-336

[8] Das, Manab K. and Ghoshdastidar, P.S., 1994b, "A Quasi Three-Dimensional Computer model of Flow and Conjugate Heat Transfer in the Metering section of a Single-screw Plasticating Extruder.", *Proc. ASME/AIAA Thermophysics and Heat Transfer Conference, Colorado Springs, Colorado, June 20-23, HTD*-Vol.275, pp.123-133.

[9] Das, Manab K. and Ghoshdastidar, P.S., 1996, "A Quasi Three-Dimensional Computer model of Thermal Transport Process in the Metering section of a Single-screw Plasticating Extruder.", *Communicated.*

[10] Fenner, R T., 1977, "Developments in the Analysis of Steady Screw Extrusion of Polymers", *Polymer,* Vol.18, pp.617-635.

[11] Fenner, R T., 1980, *Principles of Polymer Processing*, Chemical Publishing, New York.

[12] Fischer, E G., 1954, *Extrusion of Plastics.*, Illife Books Ltd., London.

[13] Fricke, A.L., Clarke, J.P. and Mason T.F., 1977, "Cooking and Drying of Fortified Cereal Foods Extruder Designs", *Chem. Eng. Prog. Symp. Ser. 73163*, p.134.

[14] Fong, Daniel S C., 1978, *Experimental Study of Extrusion-Cooking of Defatted Soy Flour*, M.S. Thesis,Chemical Engineering, Virginia Polytechnic Institute and State University, U.S.A.

[15] Griffith, R.M., 1962, "Fully Developed Flow in Screw Extruders", *Ind. Eng. Chem. Fundam.* , Vol.1, No.3, pp.181-187.

[16] Gupta, M., Kown, T., and Jaluria, Y.,1992,"Multivariant Finite Element for Three-dimensional Simulation of Viscous Incompressible Flows", *Int. J. Numer.Meth. Fluids*, Vol. 14, pp.557-585.

[17] Harmann, D.V. and Harper, J.M., 1974, "Modelling a Forming Food Extruder", *J. Food Sci.*, Vol. 39, p.1099.

[18] Harper, J.M., 1978, *Extrusion of Foods*, CRC Press.

[19] Harper, J.M., Rhodes, T.P., and Waninger, L.A., 1971, "Viscosity models for Cooked Cereal Doughs", *CEP Symp. Ser. 67,* Vol.40, p.108.

[20] Hohner, G.A., 1978, "Quaker Oats Co.", private communication to J.P. Clark.

[21] Karwe, M.V. and Jaluria, Y., 1990 , "Numerical Simulation of Fluid Flow and Heat Transfer in a Single-screw Extruder for non-Newtonian Fluids", *Numer. Heat Transfer*, Vol.17, pp.167-190.

[22] Lawal, A. and Kalyon, D.M., 1993, "Incorporation of Wall-slip in Non-isothermal modelling of Single-screw Extrusion Processing", *1st Int. Conf. Transp. Phenom. Processing*, Technomic, Lancaster, PA.,pp.985-996.

[23] Lidor, G., and Tadmor, Z., 1976, "Theoretical Analysis of Residence Time Distribution Functions and Strain in Plasticating Screw Extruders", *Polymer Eng. Sci.*, Vol.16, pp.450-462.

[24] Marshall, D.I., Klien I., and Uhl, R.H., 1965, *SPE J.*, Vol. 21 p. 1192

[25] Martin, B. 1970, "Heat Transfer Coupling Effects Between a Dissipative Fluid Flow and it's Containing Metal Boundaries", *Report to Working Party "Non-Newtonian Liquid Processing" of the European Federation of Chemical Engineering.*

[26] Mokhtarin, F. , and Erwin, L., 1982, "Computer Analysis of Mixing in Single screw Extruders", *SPE Tech. Paper*, Vol.28, pp.476-479.

[27] Morgan R.G., Suter, D.A , and Sweat, V.E., 1978," Modelling the Effects of Temperature-time History, Shear-rate and Moisture on Apparent Viscosity of Defatted Soy Flour Dough", *Paper no. 69,* American Society of Agri. Engg., St. Joseph.

[28] Palit, K., 1974, *Some Experiments on Polymer Melt Flow in a Plasticating Extruder*, Polymer Processing Research Report No.1, Imperial College, Mechanical Engineering Department, U.K.

[29] Patankar, S.V and Spalding, D.B., 1972, "A Calculation Procedure for for Heat, Mass and Momentum Transfer in Three-dimensional Parabolic Flows", *Int. J. Heat Mass Transfer*, Vol 15, pp.1787-1806.

[30] Patankar, S.V., 1980, *Numerical Heat Transfer and Fluid Flow,* Hemisphere, Washington D.C.

[31] Raithby, G.D., and Schneider, G.E., 1979, "Numerical Solution of Problems in Incompressible Fluid Flows-Treatment of the Velocity-Pressure Coupling", *Numerical Heat Transfer*, Vol.2, pp.417-440.

[32] Remsen, C.H. and Clark J.P., 1978, "A Viscosity Model for a Cooking Dough",*J. Food Process Engineering 2,* Vol.1, pp.39-64.

[33] Rogers, M.G., 1970, " Rheological Interpretation of Brabender Plasticorder (Extruder Head) data", *Ind. Eng. Chem. Process Des. Dev.*, Vol.9(1), p.49.

[34] Roller, 1979, "Characterisation of the Time Temperature-viscosity Behaviour of Curing β-Staged Epoxy Resins",*Polymer Engg. Sci. 15,* vol 6, p.406.

[35] Rowell, H.S. and Finlayson, R.D., 1992, Engineering, p.114 and p.606.

[36] Sastrohartono, T., Jaluria, Y., Esseghir, M. and Sernas, V., 1995, "A Numerical and Experimental Study of Three-dimensional Transport in the Channel of an Extruder for Polymeric Materials", *Int. J. Heat Mass Transfer*, Vol.38, No.11, pp.1957-1973.

[37] Schlichting, H., 1979, *Boundary Layer Theory*, McGraw Hill, New York.

[38] Schwartzberg, H.G., 1979, *Food Extrusion*, FPBE News, AIChE.

[39] Singh, R.P.(Ed.), 1978, *Handbook of Physical Properties of Food Stuffs*, Marcel Dekker, New York.

[40] Tadmor, Z. and Klien, I., 1970, *Engineering Principles of Plasticating Extrusion*, Van Nostrand Reinhold Co., New York.

[41] Tadmor, Z., and Gogos, C., 1979, *Principles of Polymer Processing* , John Wiley and Sons, New York.

[42] Tsao, T.F. Harper, J.M. and Repholz, K.M., 1978, " The Effects of Screw Geometry on Extruder Operational Characteristics", *AIChE Symp. Ser. 74(172)*, p.142.

[43] Vandoormal, J.P, and Raithby, G.D., 1984, "Enhancements of the Simple Method for Predicting Incompressible Fluid Flows", *Numerical Heat Transfer* , Vol.7, pp.147-163.

[44] Zamodits, H.J. and Pearson, J.R.A., 1969, "Flow of Polymer Melts in Extruders", Part 1, The Effect of Transverse Flow and of Superposed Temperature Profile, *Trans. Soc. Rheol.*, Vol.13, No.3, pp.357-385.